

MASS-MOVEMENT EVENT STRATIGRAPHY IN LAKE ZURICH: A RECORD OF VARYING SEISMIC AND ENVIRONMENTAL IMPACTS

STRASSER, M., and F. S. ANSELMETTI (2008): Mass-movement event stratigraphy in Lake Zurich; A record of varying seismic and environmental impacts, *Beiträge zur Geologie der Schweiz, Geotechnische Serie*, vol. 95, pp. 23–41, Schweizerische Geotechnische Kommission, Zurich, Switzerland.

Abstract

Combining basin-wide high-resolution seismic imaging with coring in perialpine Lake Zurich (Switzerland) reveals a chronological catalogue of Late Glacial-to-Holocene mass-movement units, documenting a complex history of varying tectonic and environmental impacts affecting the lake and its surrounding. A total of 149 mass-movement deposits have been identified and mapped with a dense grid of seismic profiles ~300 km in length. They are allocated to 21 seismic stratigraphic event horizons, each of which comprising 1–23 individual mass-movement deposits. An age model based on information from previous studies, 6 new long piston cores and 15 new AMS-¹⁴C ages allowed establishing a well-constrained chronological mass-movement event catalogue covering the last ~17000 years. Results include the documentation of 3 major (2210, 11600, 13760 cal yr. B.P.) and 2 minor (640 and 7270 cal yr. B.P), simultaneously-triggered basin-wide lateral slope failure events interpreted as the fingerprint of paleo-seismic activity in the Zurich area. Furthermore, two major slide events were discovered, which occurred during the transition from the Pleniglacial to the Late Glacial time period and thus are likely related to the activity of the nearby Linth glacier. Additionally, our record reveals higher frequency of Holocene mass movements in deltaic settings during specific periods that may be related to climate-controlled increase of sediment supply, supposing climatic causing factors for subaqueous delta slope failures. These findings thus point at a variety of potentially hazardous processes, such as earthquakes, lake outbursts and floods, that affected the Zurich area over the last ~17000 years.

Zusammenfassung

Hochauflösende reflexionsseismische Profile, welche den Untergrund des schweizerischen Zürichsees beckenweit abbilden, und Sedimentproben an gezielt ausgewählten Kernlokalitäten erlauben es, Spätglaziale und Holozäne Ablagerungen subaquatischer Massenbewegungen im See räumlich und zeitlich auszukartieren. Der somit erfasste Ereigniskatalog lässt auf eine Vielzahl unterschiedlicher geologischen, tektonischen und klimatologischen Einflüsse schliessen, welche in der Vergangenheit auf den See und auf dessen Umgebung eingewirkt haben müssen.

In den ~300 km umfassenden seismischen Profilen, welche in einem engmaschigen Gitter über den See verteilt aufgenommen wurden, lassen sich total 149 einzelne Massenbewegungsablagerungen kartieren. Diese finden wir in 21 stratigraphischen Niveaus (i.e. seismostratigraphische Ereignishorizonte), welche jeweils 1–23 individuelle Ablagerungen umfassen. Mit Hilfe von Informationen aus früheren Studien und 6 neu abgeteufte Kolbenlotkernen, an welchen insgesamt 15 neue Radiokarbondatierungen (¹⁴C) durchgeführt wurden, lässt sich ein hochauflösendes Altersmodell der Sedimentationsgeschichte im See erstellen. Daraus ergibt sich die Chronologie der Massenbewegungsereignisse im Zürichsee über die letzten ~17000 Jahre. Die Studie dokumentiert 3 grosse (2210, 11600, 13760 Jahre vor heute) und 2 kleinere (640 und 7270 Jahre vor heute) Ereignisse, welche durch gleichzeitig ausgelöste, beckenweite Rutschungen entlang der seitlichen Unterwasserabhängen charakterisiert sind, und welche als Zeugen vergangener Erdbebenaktivität im Raum Zürichsee interpretiert werden. Im Weiteren wurden zwei grossräumige Versackungs- und Massenbewegungsereignisse während des endeiszeitlichen Gletscherrückzugs entdeckt, welche wohl im Zusammenhang mit der Aktivität des damals nahegelegenen Linth Gletschers stehen dürften. Entlang von Deltaabhängen konnten nacheiszeitliche Hanginstabilitäten während bestimmten Zeitintervallen nachgewiesen werden, welche möglicherweise mit Klimaphasen zusammen fallen, die zu einem erhöhtem Sedimenteintrag in den See führten. Dies lässt einen klimatischen Kontrollfaktor für die Stabilität von subaquatischen Deltaabhängen vermuten.

Die Resultate der Studie dokumentieren somit das Auftreten verschiedener geologischer Ereignisse, wie Erdbeben, Seeausbrüche oder Hochwasser, welche sich im Verlaufe der letzten rund 17000 Jahren in der Zürichsee Region ereignet haben und welche, aus heutiger Sicht betrachtet, mögliche Naturgefahren darstellen könnten.

3.1 Introduction

Subaqueous mass movements such as slides, slumps, mass flows and turbidity currents are important players for sediment transport and redeposition mechanism in both marine and lacustrine environments. They also pose societal and environmental risks to offshore infrastructures (e.g. pipelines, cables and platforms) as well as to coastal areas (e.g. due to shore collapses and landslide-induced tsunamis) (CAMERLINGHI et al, 2007). Mass flows and turbidity currents often evolve from mass-failure processes along the submerged sediment-covered slopes (e.g. translational or rotational slides) that may originate from various processes including rapid sedimentation, gas release or migration, earthquake shaking, glacial and tidal loading and wave action (HAMPTON et al, 1996; MULDER & COCHONAT, 1996; LOCAT & LEE, 2002). Some of these geological processes act on the submerged slopes over longer periods whereas others are of instantaneous nature (e.g. earthquakes). Studying the geological record of subaquatic mass-movement deposits, determining and characterizing their type, distribution and frequency as well as deciphering their causes and effects, thus may reveal important information to evaluate the geo-hazard potential arising from such processes.

Lakes provide ideal sedimentary archives to track such processes, as lacustrine deposits usually are spatially and temporally continuous (e.g. STURM & LOTTER, 1995). This allows investigation on a basin-wide scale and offers a well-constrained age control. Characteristic mass-movement event beds in lake sediments have been allocated to historically described catastrophic events, including earthquakes (e.g. SHILTS & CLAQUE, 1992; CHAPRON et al., 1999; SCHNELLMANN et al, 2002; 2006), human-induced shore collapses (e.g. KELTS & HSÜ, 1980; HSÜ & KELTS, 1985; LONGVA et al., 2003) and delta failures (e.g. SIEGENTHALER & STURM, 1991). Based on the fingerprints of such historic events in «recent» sediments, similar prehistoric events can be recognized in the sedimentary archive (e.g. SCHNELLMANN et al., 2002; 2006; SLETTEN et al., 2003; STRASSER et al., 2006) and allow for evaluating recurrence times of related geological impacts that often exceed the time span covered by historical archives.

However, the here studied perialpine Lake Zurich (Switzerland) was so far not specifically investigated for studying prehistoric subaqueous mass movements and for exploring their related geological processes. In this study, the presented combined basin-wide high-resolution reflection seismic and coring approach aims (i) to identify and date Late Glacial-to-Holocene mass-movements deposits, (ii) to characterize their types and distribution, (iii) to determine the associated depositional, transport and slope-failure trigger mechanism(s), and (iv) to establish a chronological catalogue of past mass-movement events, which eventually provides the basis to (v) discuss impact and frequency of various potentially-hazardous natural processes that affected the Lake Zurich area over the last ~17000 years.

3.2 Geological setting and previous studies

Lake Zurich occupies a perialpine, glacially overdeepened, NW-SE trending trough situated in the northern part of the Swiss Plateau (Fig. 3.1). It can be divided into two basins that are carved into mainly flat-lying sandstones, siltstones and marls of the Tertiary «Obere Süswasser Molasse» (OSM) formation. The general morphology consists of (i) a north-western, elongated deep basin (max water depth 135 m) with steep lateral slopes and a flat basin plain, and (ii) a flat and shallow (~20 m water depth), sediment-filled upper basin, which is divided from the lower basin by a sediment-covered subaqueous rock barrier showing a complex, step-like morphology descending towards NW (HSÜ and KELTS, 1970; SCHINDLER, 1976) (hereafter termed «escarpment structure»). A mostly sub-aerial sill formed by the Hurden Moraine between Rapperswil and Pfäffikon with only 2 m deep lake passages separates Lake Zurich in the northwest from Obersee in the east. Note that Obersee often also is referred to be a part of Lake Zurich. In this study, however, «Lake Zurich» only comprises the lower deep and the upper flat and shallow basins, whereas Obersee is treated as separate lake.

The main rivers (Linth, Jona, and Wägitaler Aa), contributing about 90 % of Lake Zurich's water supply, discharge into Obersee, which acts as the dominant sink for the clastic sediment supply from the mainly alpine catchment. During the Late Glacial period, the Sihl river temporarily discharged into the lower Lake Zurich basin depositing a large, nowadays inactive delta (HUBER, 1938; SCHINDLER, 1968), which, together with the moraine from the Zurich Stadium, borders the lake on its northwestern margin (Fig. 3.1). Since Early Holocene times, the here studied Lake Zurich lacks major active deltas and, as a consequence, shows relatively low sedimentation rates. However, local creeks laterally entering the lake contribute to Lake Zurich's clastic sediment supply and form small local deltas along the shorelines (e.g. deltas of Küsnacht, Erlenbach, Meilen and Horgen/Käpfnach; Fig 3.1). Lake level during that time generally was stable and only oscillated by max. 2–3 m corresponding to climatic variations, precipitation pattern and Sihl river sediment discharge that may have influenced the Limmat river outflow situation (SCHINDLER, 1971; MAGNY, 2004; RIESEN and NEAF, 2007).

Several previous studies in the 1970's and 1980's described Lake Zurich's geology and its sedimentary and environmental evolution since the Last Glacial Maximum (HSÜ and KELTS, 1970; 1984; SCHINDLER, 1974; 1976; KELTS, 1978; GIOVANOLI, 1979; PIKA, 1983; LISTER, 1985; 1988; SIDLER, 1988). These studies are mainly based on data from the deep northwestern basin comprising some seismic lines and piston cores, and one deep drill hole termed «Zübo» (see HSÜ and KELTS, (1984) and references therein). These data reveal that in the lower Lake Zurich basin, the molassic bedrock is covered with an up to 140 m-thick, mainly glacial and glacio-lacustrine infill. The majority of these sediments were accumulated in a subglacial environment. Only the uppermost ~30 m were deposited after the glacier retreated from the lower Lake Zurich basin (see lithostratigraphic description in subsection 3.4.2.1).

In this upper sedimentary succession, none of the previous studies specifically addressed interpretation and correlation of Late Glacial-to-Holocene mass-movement deposits throughout the lake. Only a series of subaqueous slumps on the shore near Horgen that occurred in 1875 A.D. was extensively studied and described by HEIM (1976), KELTS (1978), KELTS & HSU (1980) and SIEGENTHALER et al. (1984). Additionally, shore collapses near Rüslikon in 1898, 1900 and 1907, near Oberrieden in 1918 and near Küsnacht in 1943 and 1955 were mentioned in the literature (e.g. NIPKOW, 1920; KUEN, 1999). All these slopes instabilities resulted directly from human-induced loading of sand and gravel landfill on a weak foundation of lacustrine chalk. These shore collapses and slumps resulted in mud-flow and mud-flow-evolved turbidite deposits that can be traced in the sedimentary record throughout the lower Lake Zurich basin (KELTS, 1978; PIKA, 1984).

3.3 Methods

With the objective to identify, characterize, map and date Late Glacial-to-Holocene mass-movement deposits, the existing sedimentary model of the postglacial infill of Lake Zurich was refined by acquiring new high-resolution seismic reflection data and 6 new long sediment piston cores (Fig 3.2). Additionally, a sidescan-sonar survey covering a limited area offshore Oberrieden aimed to characterize the lake floor surface expression and spatial geometry of a prominent sub-recent mass-movement deposit.

3.3.1 Reflection seismic subsurface imaging and seismic stratigraphic mapping

A dense grid of ~300 km of single channel 3.5 kHz seismic profiles (acoustic pinger source) was acquired to image the subsurface in quasi 3-D. The source/receiver was mounted on a catamaran that was pushed in front of a small vessel. DGPS-positioning with a maximum error of ± 2 m guaranteed accurate navigation. The digitally-recorded data were processed using a flat gain and a band-pass filter. Two-way travel time was converted to water depth and sediment thickness using a constant velocity of 1450 ms^{-1} .

Landslide deposits in the seismic data were identified based on characteristic chaotic to transparent seismic facies that contrasts with continuous reflections produced by regular, undisturbed sediments (see subsection 3.4.1.2). The top of each mass-movement deposit was defined at its pinch-out point and assigned to a distinct «event horizon» (i.e. seismic stratigraphic horizon related to at least one mass-movement deposit (SCHNELLMANN et al, 2006)). Such horizons represent isochrons that can be traced throughout the entire lake basin, establishing a basin-wide catalogue of mass-movement deposits and allowing recognition of synchronous landslide events.

3.3.2 Sidescan-sonar imaging

Offshore Oberrieden, a limited lake floor area was imaged using a digital dual frequency (100/325 kHz) sidescan-sonar

system (C-Max sidescan with a 760 CodaOctopus acquisition system). The fish was deep-towed maintaining a constant fish-to-lake floor offset of ~15 m and a constant boat speed along parallel track lines to obtain a uniform spatial footprint without distortion. The digitally-recorded data of each single track was processed using slant-range and signal-attenuation corrections implemented in the processing software (Octopus 461 Processing Toolkit). For positioning of the lake floor images, the layback of the fish has been calculated by matching the positions of acoustically prominent lake floor features imaged in two parallel lines that advance in opposite directions. Resulting images of single track lines were exported and manually mosaiced using Adobe Photoshop.

3.3.3 Coring and dating

Six Kullenberg-type gravity piston cores (KELTS et al., 1986), each 8–10 m in length, were recovered at key positions to groundtruth the seismic data, for detailed sedimentological analyses and dating. The cores were scanned with a GEOTEK multisensor core logger, which measures gamma ray attenuation bulk density, compressional wave velocity and magnetic susceptibility. Afterwards, cores were split, photographed and sedimentologically described (macroscopically and using smear slide techniques). Accelerator mass spectrometry ^{14}C analysis on terrestrial organic matter (ideally leaf fragments to minimize the risk of dating reworked material) sampled at different stratigraphic levels in four cores were performed at the Particle Physics Laboratory of ETH Zurich to date the sedimentary succession. Radiocarbon ^{14}C -ages were calibrated using the IntCal04 calibration curve (REIMER et al., 2004). In addition, core and age information from previous studies (KELTS, 1978; GIOVANOLI, 1979; PIKA, 1983; LISTER 1988; SIDLER, 1988) were incorporated using core-to-core and seismic-to-core correlation. Non-calibrated radiocarbon ages given in these previous studies were also calibrated (REIMER et al., 2004), so that all ages in this study refer to the same time scale.

For dating an individual event horizon the lithostratigraphically closest 1–4 ^{14}C -ages were selected (in different cores, if possible). The error introduced by the offset between the lithostratigraphic position of ^{14}C -ages and the event horizon was corrected using the estimated sedimentation rates applied to the sample-horizon offset. Sedimentation rates were estimated for each individual core by linearly interpolating between two ^{14}C samples after correcting for the thickness of instantaneously deposited turbidite layers. For each of the 1–4 selected samples an age range for the event horizon then was calculated. Subsequently, the overlap of the obtained age-ranges and its center was determined. The same procedure was repeated for each of the event horizons. Additionally, counting of sediment laminations in lithostratigraphic Unit 1a and 1b (see subsection 3.4.2.1) that have been interpreted as varve couplets by GIOVANOLI (1979), ZAO (1984), and NIESSEN et al. (1992), as well as age information based on geomagnetic correlations (BASTER, 2002) were used to refine the estimated sedimentation rates and resulting age model for the sedimentary succession prior to ~14000 cal yr B.P..

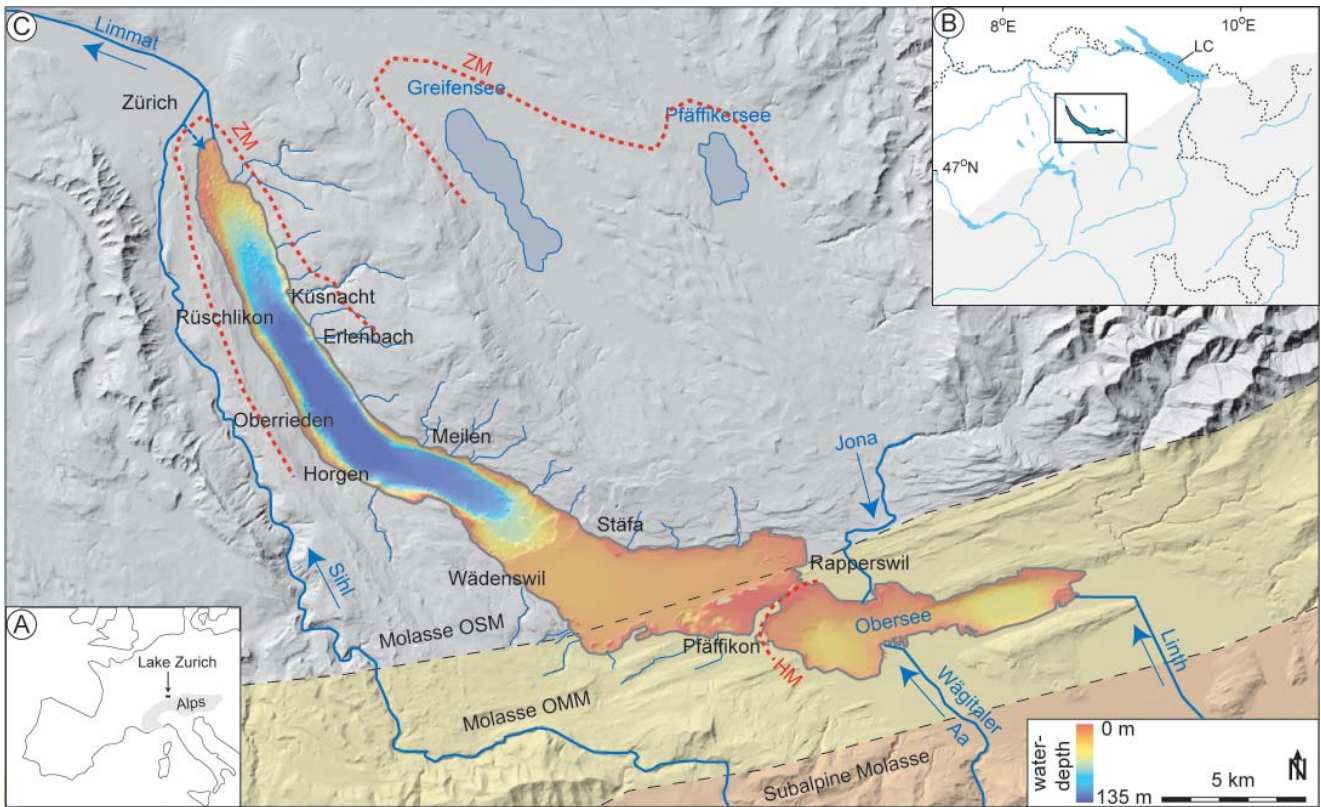


Figure 3.1: Geographic location of Lake Zurich: A) location with respect to Europe and the Alpine chain (gray shaded area). B) Close up view showing the Alps (gray shaded area) and the northern Swiss Plateau (white area). Dotted lines mark country borders of Switzerland, Germany, Austria, Liechtenstein and Italy. Rectangle indicates position of Fig. 3.1C. LC = Lake Constance. C) Lake Zurich's and Obersee's colored bathymetric map embedded in its geographic and geological context. Dashed red lines show prominent geomorphic features resulting from retreatal moraines that were formed during overall glacier retreat (ZM = Zurich Moraine, HM = Hurden Moraine). Blue arrows and annotations indicate flow direction and major rivers, respectively. Background: Shaded relief of digital elevation model (dhm25, Swisstopo) overlain by the general geological setting (OSM = Obere Süswasser Molasse; OMM = Obere Meeres Molasse).

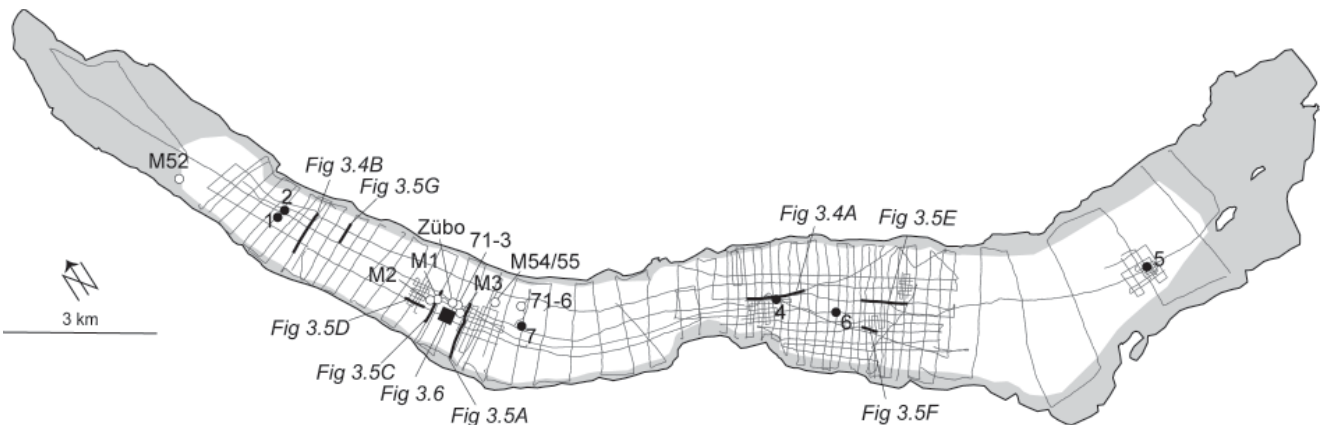


Figure 3.2: 3.5 kHz seismic survey grid in Lake Zurich and location of cores. Black dots and open circles indicate positions of new cores ZHK04-1 to 7 (this study) and from previous studies (KELTS, 1978; GIOVANOLI, 1979; PIKA 1983; LISTER, 1988; SIDLER 1988), respectively. Solid black lines mark locations of seismic lines shown in subsequent figures. Gray shaded areas indicate marginal areas where the acoustic signal did not penetrate into the subsurface. Black square marks location of sidescan-sonar survey area and map shown in Figure 3.6.

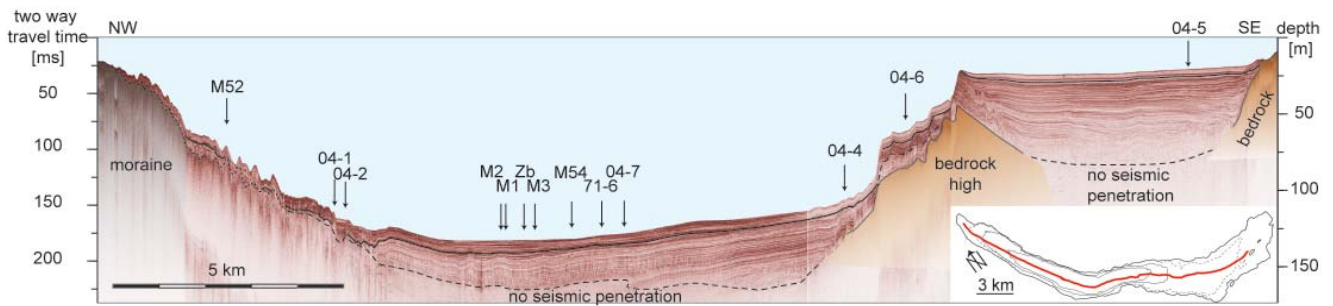


Figure 3.3: 3.5 kHz reflection seismic profile (pinger source) imaging the subsurface of Lake Zurich along the whole longitudinal lake axis with projected locations of cores shown in Figures 3.7 and 3.8. Black line in the seismic data corresponds to the boundary between seismic stratigraphic Unit A below and Unit B above. Inlet in the lower right corner shows location of the seismic line (solid red line). Contour interval is 50 m. Dotted contour line marks 20 m-depth contour line and aims to clarify basin morphology in the upper flat basin.

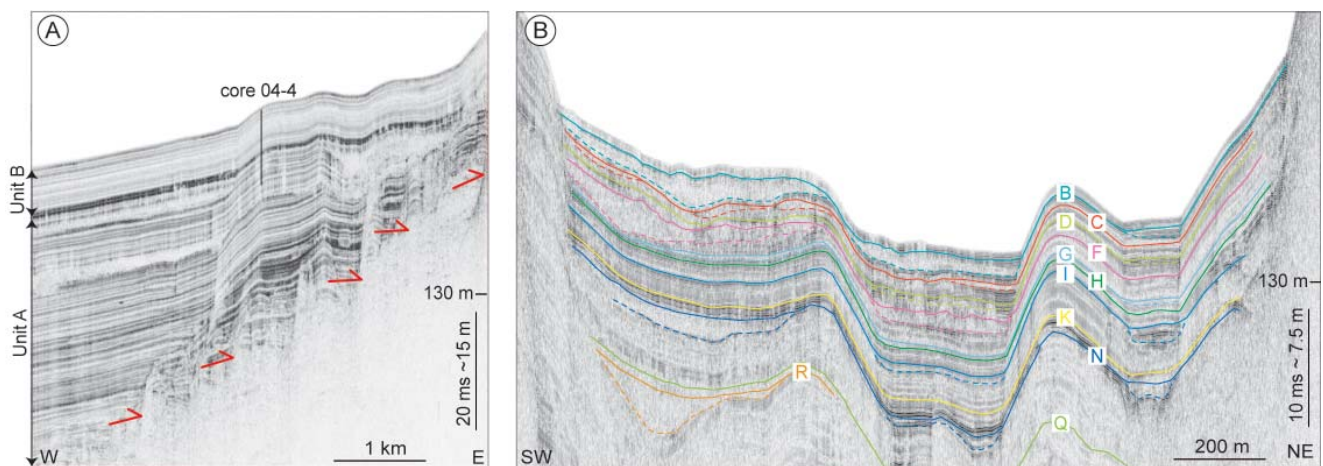


Figure 3.4: 3.5 kHz reflection seismic profiles illustrating general features of the seismic stratigraphy of Lake Zurich. See Figure 3.2 for location of seismic lines. A) Seismic section illustrating the two distinct differences in the geometry-style (ponding vs. draping) of Unit A and B, respectively. Red arrows indicate onlap patterns. A coring site is indicated with a vertical solid black line. B) Seismic line perpendicular to the lake axis in the northwestern part of Lake Zurich illustrating stacked mass-movement deposits of a few 10's to 100's of meters horizontal extension with internal chaotic-to-transparent seismic facies and clear lateral pinch-out geometries. Different-colored solid lines mark seismic stratigraphic horizons relating to the top of individual mass-movement deposits (i.e. event horizons B to R). Dashed colored lines mark the base of individual mass-movement bodies. The thin package of coherent, high-amplitude reflections between event horizons N and K corresponds to the transition zone between seismic stratigraphic units A and B.

3.4 Data and Results

3.4.1 Reflection seismic data

3.4.1.1 Seismic stratigraphy

Two seismic stratigraphic units can be identified in the seismic data that image ~50 and ~75 ms or the upper ~35 and ~60 m of the sedimentary infill of the lower and the upper basin, respectively (Fig. 3.3). In the deep basin the two seismic units are separated by a thin package (0.5 to 1 m thick) of coherent, high-amplitude reflections (Fig. 3.4A). The two seismic units are characterized as follows:

- (i) The seismic Unit A comprises a thick (~15 to 25 m and up to 55 m in the lower and upper basin, respectively) succession of acoustically stratified sediments characterized by parallel reflections of varying amplitudes. Towards the basin margins, the vertical amplitude variations are more closely spaced and the reflections often onlap onto the acoustic basement, indicating a dominant ponding-style of sedimentation (Fig. 3.4A).
- (ii) The overlying seismic Unit B (~5 to 7 m thick) is characterized by closely-spaced, parallel reflections of medium-to-high and low-to-medium amplitudes

in the lower and the upper basin, respectively. Unit B forms a drape across the entire basin generally also covering the slopes. However, the drape is absent on the uppermost ~ 20 m-high scarp where glacio-lacustrine deposits outcrop along the escarpment structure (Boner et al., 1999) and moat features suggest current-induced erosion and/or non-sedimentation (Fig. 3.5E).

3.4.1.2 Types of mass-movement deposits

Sedimentary bodies of a few 10's to 100's of meters horizontal extension with internal transparent to chaotic-to-transparent seismic facies and clear lateral pinch-out geometries can be identified throughout the sedimentary succession in the lower basin and along the escarpment structure (Figs. 3.4B and 3.5). On the basis of different geometries, seismic facies and geographical occurrence, four different types of mass-movement deposits can be distinguished. They are described in the following section, which also delineates the interpreted transport and depositional mechanism associated to these types of mass-movement deposits.

Mass-flow deposits resulting from translational sliding along lateral steep slopes

The most prominent mass-movement deposits identified in the study area occur in the lower basin close to the slope breaks and are characterized by basinward-thinning bodies with distinct distal terminations, a transparent to sometimes partly chaotic-to-transparent seismic facies and generally smooth top surfaces (Figs. 3.4B, 3.5A, C and D). These observed geometries and seismic facies are typical characteristics of subaquatic mass-flow deposits (e.g. PRIOR et al, 1984; MULDER & COCHONAT, 1996; SCHNELLMANN et al. 2006) and indicate mass transport from the 15–20° steep lateral slopes towards the basin. Along the lateral slopes, failure scars related to the mass-flow deposits can be identified in seismic profiles (Figs. 3.5A and B). They reach > 5 m in height and generally occur on steepening-downwards slopes in water depth > 40 m. Observed geometries indicate translational sliding of the whole sedimentary drape covering the slopes along a basal gliding plane. A short gravity core recovered along the eroded slope offshore Oberrieden (i.e. slope failure event associated to the mass-flow deposit shown in Figures 3.5C and D) revealed that the sliding plane consists of glacial deposits and indicate comparable characteristics as described for lateral slope failures in Lake Lucerne (STRASSER et al., 2007).

In Lake Zurich mass-flow deposits that evolved from translational sliding along the steep lateral slopes reach thicknesses of 1 to 7 meters and cover areas of a few 10's to 100's of meters horizontal extension. Seismic profiles crossing thick mass-flow deposits often indicate that the chaotic-to-transparent seismic facies reaches deeper than the mass-flow deposit itself indicating deformation of the overridden basal basin-plain sediments. This deforma-

tion sometimes is visualized by steeply dipping, high-amplitude reflections/diffractions in the frontal part of the acoustically chaotic-to-transparent bodies (Fig. 3.5C) suggesting frontal thrusting as the result of an adjustment of the underlying sediments to the increased static and dynamic loading during mass-flow deposition (SCHNELLMANN, 2005). Sidescan-sonar data of a sub-recent lateral mass-flow deposit offshore Oberrieden show arcuate frontal compressional ridges associated with the mass-movement deposit (Fig. 3.6), supporting the interpretation of gravity spreading induced by loading of the slope-adjacent lake floor during lateral mass-flow deposition.

Mass-flow deposits resulting from rotational sliding along the escarpment structure

A second type of acoustically transparent mass-flow deposits was identified in the seismic data at the toe and in the intermediate sub-basins of the step-like escarpment structure (Fig. 3.5E). They only occur within seismic Unit A. On the basis of their geometries they clearly indicate mass-transport direction parallel to the lake axis. The source area of these mass movements thus is interpreted to be situated along the upper scarps of the escarpment structure. However, complex geometries and potentially current-induced erosion and/or non-sedimentation as indicated by moat structures and outcropping of glacio-lacustrine deposits along the uppermost ~ 20 m-high scarp (BONER et al, 1999) (Fig. 3.5E) mask clear indicators of slope failure processes associated with this type of mass-flow deposition. Nevertheless, few seismic lines indicate rotational slide blocks associated with these mass-flow deposits (Fig. 3.5F), which thus are interpreted to have evolved from rotational sliding along the escarpment structure.

Wedge-shaped mass accumulation bodies in distal deltaic areas

Apart from the well-defined mass-flow deposits described above, seismic data in distal areas of small lateral deltas often show small wedges that taper off towards the basin. They generally comprise one to 3 low-amplitude reflections that downlap on a single seismic stratigraphic horizon in a basinward direction (Fig. 3.5G). No single mass-movement can be assigned to such wedge-shaped bodies because seismic penetration often is limited in delta-proximal areas and individual remobilization events along the delta supposedly are too small to be resolved on seismic sections. Therefore, these depositional units mapped as the correlated seismic stratigraphic horizons rather represent a series of individual small events and are interpreted to indicate periods of increased mass accumulation in the distal part of small lateral deltas resulting from small-scale remobilization on the steep delta slopes (e.g. mass flows induced by delta front collapses) and partially from higher clastic input from small creeks laterally entering Lake Zurich (see subsection 3.5.3).

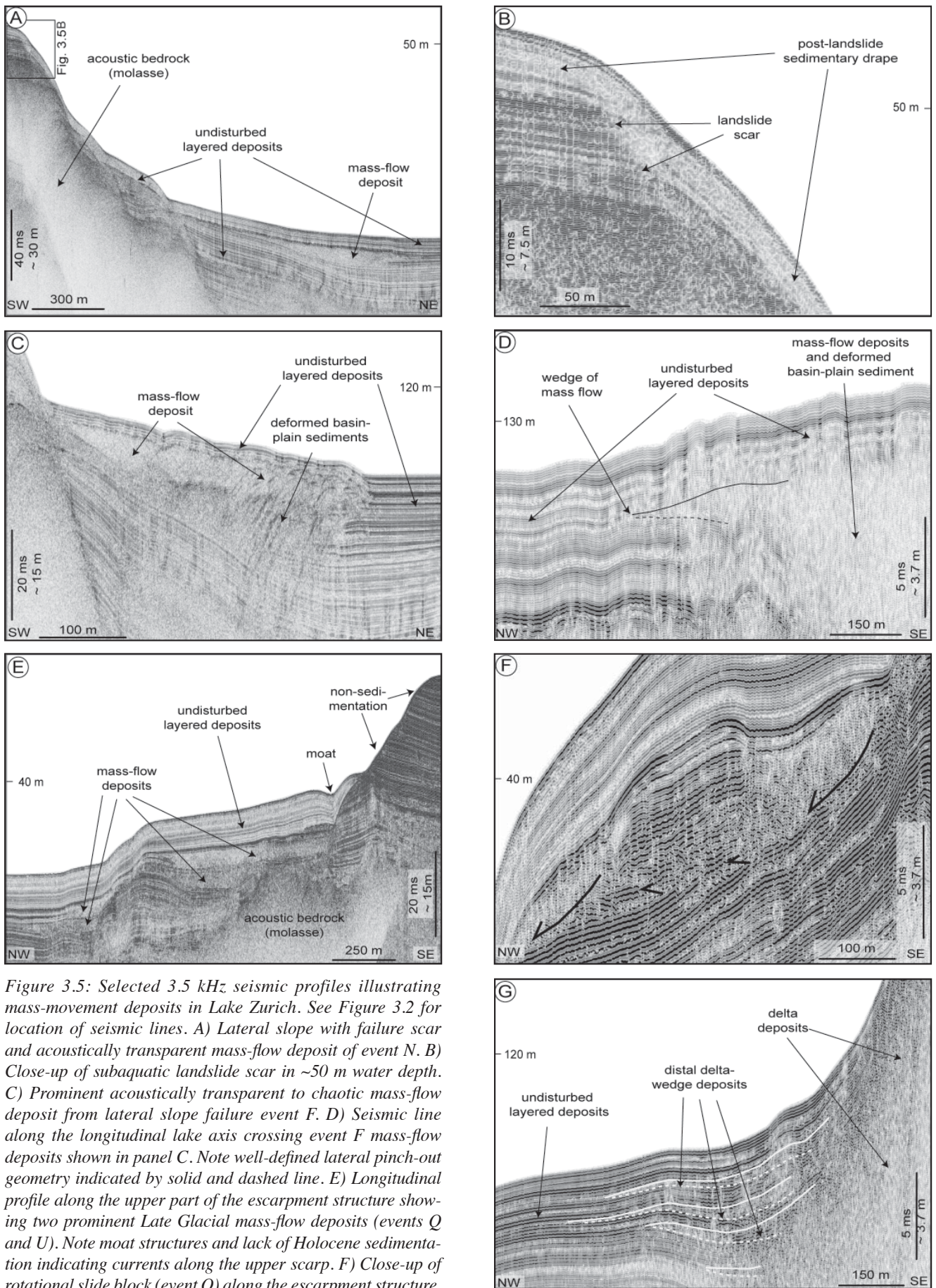


Figure 3.5: Selected 3.5 kHz seismic profiles illustrating mass-movement deposits in Lake Zurich. See Figure 3.2 for location of seismic lines. A) Lateral slope with failure scar and acoustically transparent mass-flow deposit of event N. B) Close-up of subaquatic landslide scar in ~50 m water depth. C) Prominent acoustically transparent to chaotic mass-flow deposit from lateral slope failure event F. D) Seismic line along the longitudinal lake axis crossing event F mass-flow deposits shown in panel C. Note well-defined lateral pinch-out geometry indicated by solid and dashed line. E) Longitudinal profile along the upper part of the escarpment structure showing two prominent Late Glacial mass-flow deposits (events Q and U). Note moat structures and lack of Holocene sedimentation indicating currents along the upper scarp. F) Close-up of rotational slide block (event Q) along the escarpment structure. G) Seismic line showing the distal part of Erlenbach Delta and mapped wedge-shaped mass accumulation bodies.

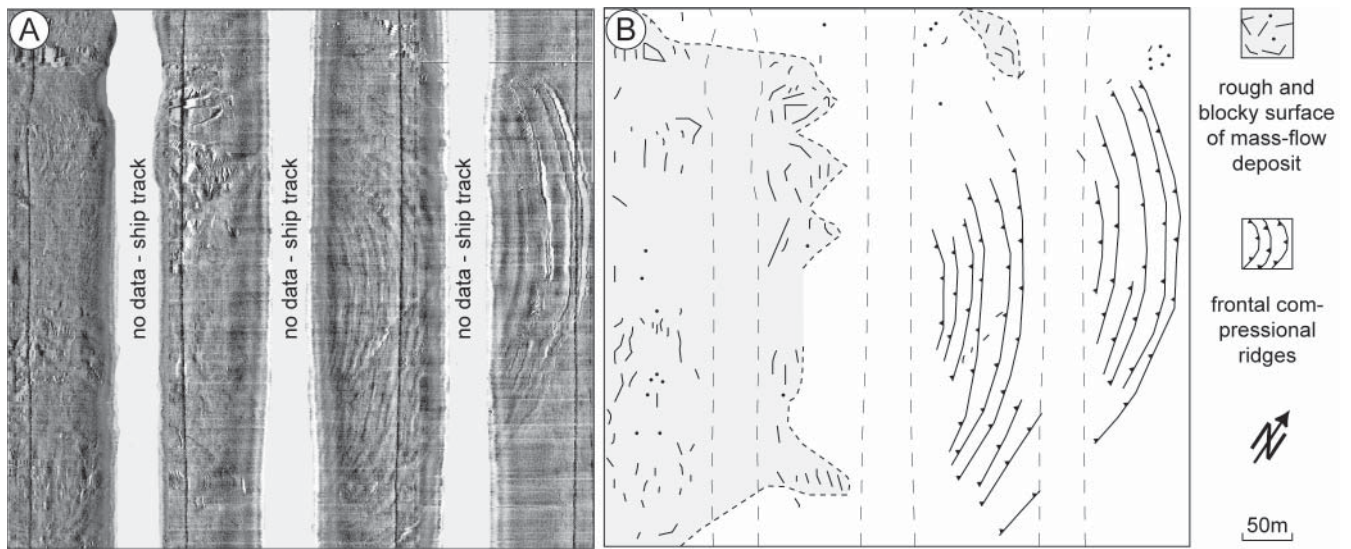


Figure 3.6: A) Sidescan-sonar image illustrating the lake floor surface expression and spatial geometry along the distal part of the 1918 A.D. Oberrieden mass-flow deposit (see Figure 3.2 for location of map segment). B) Interpretation of sidescan-sonar image showing the rough and blocky surface of the mass-flow deposit (mass-movement transport downslope from left to right) and associated arcuate frontal compressional ridges propagating into the basin plain.

Turbidite deposits

In the deepest depressions of the lower basin, event horizons assigned to mass-movement deposits often correlate to few dm to m-thick, acoustically almost transparent bodies that are characterized by smooth top surfaces and by well-defined ponding geometries. This geometry and acoustic signatures is typical for thick, extensive turbidite and homogenite deposits, which generally result from large mass flows (e.g. STURM & MATTER, 1978; HSÜ & KELTS 1985; BOUMA, 1987; SCHNELLMANN et al, 2006). In Lake Zurich, only event horizons related to larger mass-flow deposits are associated with seismically resolvable turbidite deposits. However, smaller events often are associated with seismic reflections showing higher amplitudes indicating the presence of smaller turbidite layers (see subsection 3.4.2.3).

3.4.2 Core data

3.4.2.1 Lithostratigraphy

All six newly acquired sediment cores (see Figure 3.2 for core locations) recovered the characteristic postglacial stratigraphic succession that reflects the general sedimentary and environmental evolution of Lake Zurich as already described in previous studies (KELTS, 1978; GIOVANOLI, 1979; PIKA, 1983; HSÜ and KELTS, 1984; LISTER, 1988; SIDLER, 1988). Figure 3.7 shows a compilation of all available core information from Lake Zurich. The general sedimentary succession comprises three lithologic units (from bottom to top):

Lithologic Unit 1 «glaziale Seebodenlehme» - plastic mud

Sticky, medium-gray, plastic clays to silty clays with high bulk densities showing distinct up to 5 cm-thick laminations in the lower part (U1a - laminated plastic mud), thin mm-scale laminations intercalated with yellowish, mm-scale silt to fine sand layers in the middle part (U1b - faintly laminated plastic mud) and homogenous to mottled textures in the upper part (U1c - mottled plastic mud). This lithologic unit corresponds to the upper part of seismic Unit A. Thicker laminae in deep-water cores contrast thinner laminae in shallow-water cores and thus confirm the ponding-style depositional character of this sedimentary unit. The lithology and infill pattern indicate glacio-lacustrine sedimentation by underflows in a proglacial environment. The lamination in the lower and middle part of this unit has been interpreted as varve deposits, reflecting annual pulses of suspension input from meltwater plumes of a nearby glacier (U1a) (ZAO et al, 1984) and seasonal aeolian dust sedimentation (loess) during the Oldest Dryas (U1b) (GIOVANOLI, 1979; NIESSEN 1992)

Lithologic Unit 2 «Basaler Faulschlamm» - iron sulfide mud

Dark greenish-gray clays to silty clays with low carbonate content and low bulk densities showing a distinct appearance of several highly FeS-pigmented black laminations and intercalated cm-thick sandy to silty turbidites. From its stratigraphic position, this unit corresponds to the seismic high-amplitude reflections in the transition zone between seismic Units A and B. It is interpreted that, with postglacial climatic amelioration and the final retreat of the glaciers back into the Alps, catchment erosion and runoff

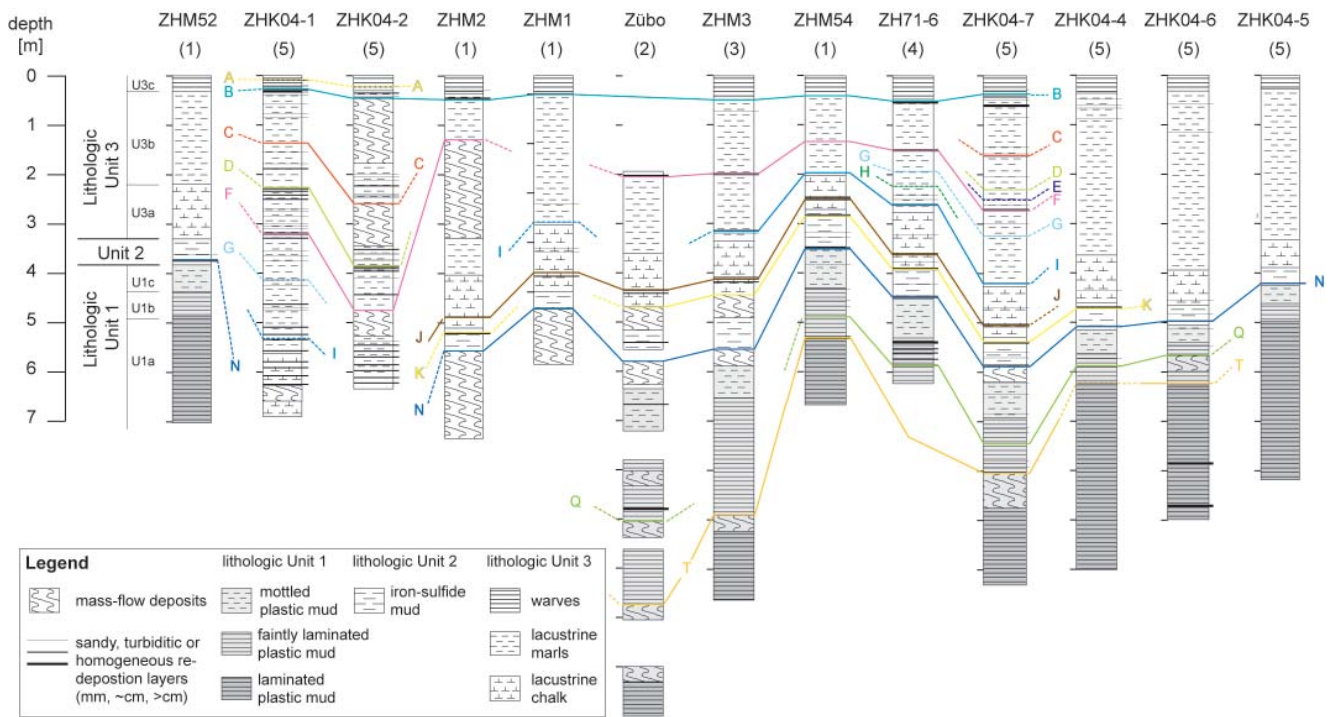


Figure 3.7: Core transect approximately along the longitudinal lake axis from NW to SE compiling all available core information from Lake Zurich ((1) GIOVANOLI, 1979, (2) LISTER, 1988, (3) PIKA, 1983, (4) KELTS, 1978, (5) this study). See Figure 3.2 for core locations. Note that core ZHK04-1 and ZHK04-2 represent sites close to Küsnacht and Erlenbach Deltas and thus show higher sedimentation rates. Core ZHM54 and ZH71-6 are from slightly elevated positions and are projected here onto the basin axis. Different-colored solid lines delineate core-to-core correlation of mass-movement horizons (i.e. event horizons A to T). Uncertain correlations are indicated with dashed lines and are mainly based on seismic-to-core correlation.

into the lake was reduced and the lake became stratified. Lacustrine biota is established and oxygen content in the bottom-water dropped occasionally to anoxic levels, resulting in characteristic FeS-pigmented black laminations of the lithologic unit (e.g. KELTS, 1978; PIKA, 1983).

Lithologic Unit 3 «Seekreide» and «Seekreide-Mergel»-lacustrine chalk and marls

Light gray (U3a) to greenish gray (U3b), faintly layered lacustrine chalk (U3a) and marls (U3b) composed of terrigenous mud rich in authigenic carbonate, intercalated with cm-thick sandy and muddy turbidites. These deposits correspond to seismic Unit B and were deposited when bio-induced calcite precipitation and minor clastic input from small local creeks were the dominant sediment sources in the mesotrophic holomictic lake. Clastic input is especially evident at two coring sites close to the Küsnacht and Erlenbach deltas, where sedimentation rates are significantly higher than in the deep basin (Fig. 3.7). Cores ZHK04-1 and 2 recovered in the distal part of these deltas show frequent 0.5 to 2 cm-thick clastic layers with high organic content. The uppermost 50 to 70 cm of lithologic Unit 3 (U3c) show distinct rhythmically layered calcite/organic couplets (varves) throughout the deep basin representing human-induced lake eutrophication after 1897 A.D. (e.g. KELTS, 1978; PIKA, 1983).

3.4.2.2 Age model

The general age model of the postglacial sedimentary infill of Lake Zurich has already been established based on few ^{14}C samples from the Zübo core (LISTER, 1988) and based on palynological data from core M54 (SIDLER, 1988). The new ^{14}C ages covering the last ~14000 years (Table 3.1) are in good agreement with these data and refine the age control since the beginning of the Bølling stage (Units 2 and 3). The new high-resolution age model established in core ZHK04-7 (Fig. 3.8) reveals Holocene ages for the lithologic Unit 3 (seismic Unit A) and Younger Dryas to Bølling ages for lithologic Unit 2.

The age model of the sedimentary succession in Unit 1 is only based on two ^{14}C ages of wood samples from the Zübo core. LISTER (1988) dated the transition U1a/U1b and U1b/U1c to 17100–18050 and 16500–17300 cal yr B.P., respectively (Tab. 3.1). Counting of rhythmites (presumably varves) in cores ZHK04-4 and 7 reveal duration of ~575 yrs (565 and 587 in cores 4 and 7, respectively) for the deposition of U1b, which is in good agreement with the relative time span estimated from the two Zübo ^{14}C samples. However, geomagnetic correlation of this interval between Lakes Zurich, Constance, Lugano and Geneva (BASTER, 2002, and references therein) consistently suggests younger absolute ages. Additional support for younger ages arises from sedimentological correlation

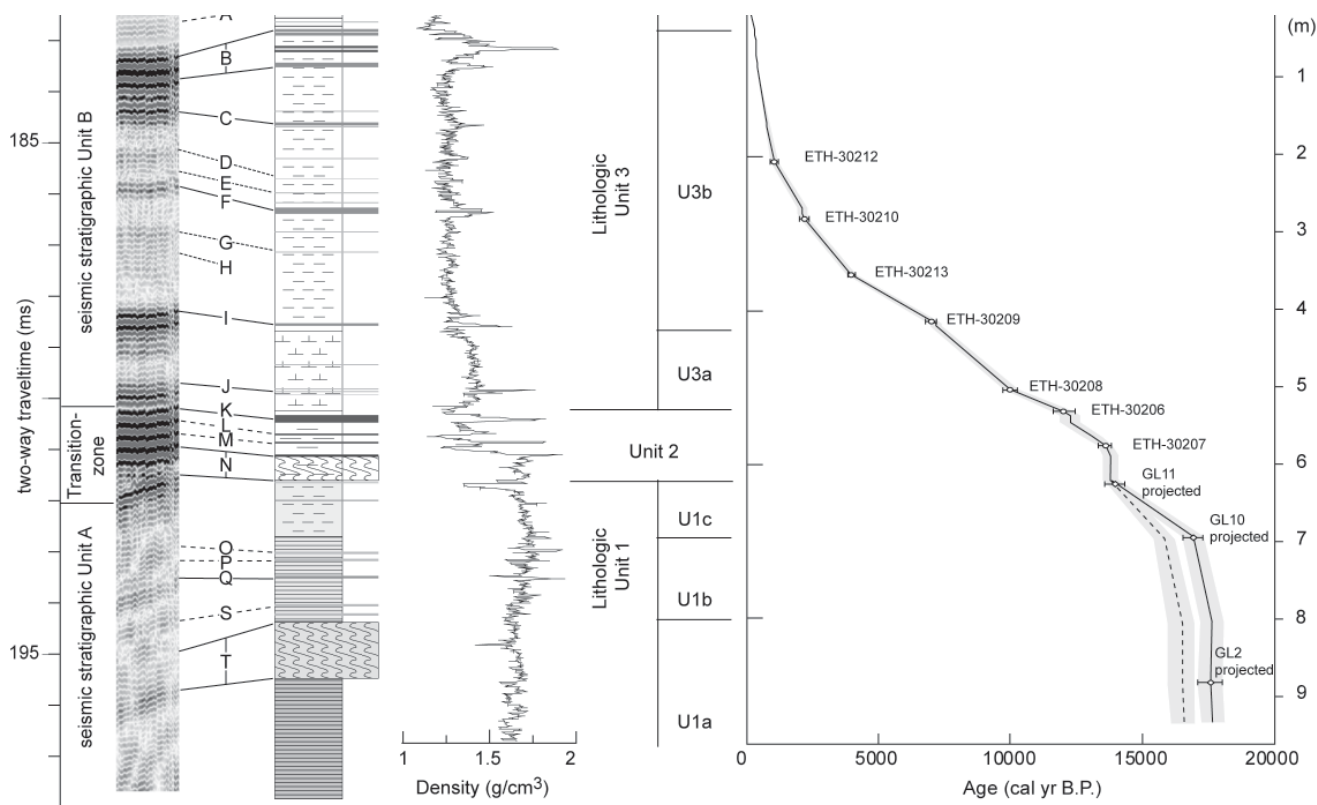


Figure 3.8: Compiled data from core ZHK04-7 (from left to right): Seismic stratigraphy at the coring site, seismic-to-core correlation, core log, bulk density log, lithostratigraphy and age model. See Figure 3.2 for core location and legend in Figure 3.7 for lithological symbols. Dashed line in the lower part of age model indicates correction for overestimated ^{14}C ages from the Zübo core (LISTER, 1988) that are projected here (see subsection 3.4.2.2 and Table 3.2). Gray area marks 2σ -range of calibrated ages.

of loess deposits recovered in several Swiss Lakes (e.g. Lakes Constance (NIESSEN et al., 1992; WESSELS, 1998) and Geneva (BASTER, 2002; GIRARDCLOS et al., 2005). Geomagnetic correlation between Lakes Zurich and Constance reveal that Lake Zurich's Units U1b and U1c (faintly laminated and mottled plastic mud, respectively) correlate to laminated loess deposits (beige-brown rhythmites) in Lake Constance (WESSELS, 1998). In his record, WESSELS (1998) counted 1370 lamination couplets between the correlated lithologic boundaries U1b/U1c and U1/U2, which suggests that U1c covers ~ 1400 years. Following this interpretation and assuming a synchronous transition, as indicated by the geomagnetic correlation, between Units U1 and U2 in both lakes (dated to ~ 14500 cal yr B.P. (Fig. 3.8 and Table 3.1)), the age model for lithologic Units U1a and U1b might be shifted by ~ 1000 (range: 650–1350) years towards younger ages (i.e. age (and range) discrepancy between Zübo date of U1b/U1c transition and correlated age in Lake Constance). Although only a first order assumption, this accounts for the (too) low sedimentation rates for U1c as estimated from the ^{14}C ages. While the Zübo ages propose that U1c sedimentation rates are in the same order of magnitude as in Unit 2 (Fig. 3.8), sediments of U1c still indicate a glacio-lacustrine sedimentation mode that clearly suggests higher sedimentation rates.

3.4.2.3 Sedimentary facies of mass-movement deposits

Mass-flow deposits

Coring the distal part of a mass-flow deposit that evolved from subaquatic translational sliding along the steep lateral slope in core ZHK04-7 recovered a characteristic succession showing a 2 cm-thick basal shear zone that is overlain by a fining upward matrix-supported mud-clast conglomerate (Fig. 3.9A). This typical mud-flow deposit is overlain by a 4 cm-thick graded turbidite layer characterized by a multiple, graded sandy to silty sequence at the base and by a homogenous clayey top layer. Similar sedimentary facies have been observed in core ZHK04-6 that recovered the distal part of a mass-flow deposit evolved from mass transport in an axis-parallel SE-NW direction along the escarpment structure. The lower part of this deposit shows a 15 cm-thick interval of heavily deformed and folded glacio-lacustrine sediments indicating slumping rather than full disintegration of the source material (Fig. 3.9B). This observation supports the interpretation that this type of mass-flow deposits evolved from rotational sliding of glacio-lacustrine sediments covering the bedrock sill in the uppermost part of the escarpment structure (see subsection 3.4.1.2).

Wedge-shaped mass accumulation bodies in distal deltaic areas

Core data from distal deltaic areas show frequent 0.5–2 cm-thick clastic layers with high organic content and sedimentation rates are significantly higher than in the central deep basin (Fig. 3.7). Seismic-to-core correlation reveals that intervals assigned to seismically imaged wedge-shaped mass accumulation bodies correspond to more frequent, thicker and coarser clastic layers (Fig. 3.9C). This observation confirms the interpretation that these wedge-shaped bodies do not represent single mass-movement events but rather periods of increased small-scale remobilization on the steep delta slopes (e.g. delta front collapses) and higher clastic input from small creeks laterally entering Lake Zurich (see subsection 3.5.3).

Turbidite deposits

A number of 1–5 cm-thick turbidite deposits have been recovered in cores retrieved in the central part of the deep basin (Fig. 3.7). In general, they show a coarser sandy to silty lower base, which sometimes comprises multiple graded sandy layers, and a fining upward sequence to-

wards a homogenous clayey top layer (Fig. 3.9D). Smaller turbidite layers, however, do not always have a graded character and sometimes comprise only a 0.5–1 cm-thick homogenous silt or clay layer and/or a thin top layer with higher organic content (Fig. 3.9E). Occasionally, amalgamation of small individual turbidite layers lacking intercalated undisturbed sediment can be observed (Fig. 3.9F). Most of the turbidite layers recovered in cores from the deep basin can be correlated to event horizons assigned to mass-movement deposits mapped elsewhere in the deep basin (Fig. 3.8). In distal deltaic areas, however, they occur more frequent and probably also represent flood-related hyperpycnal-flows deposits.

3.4.3 Catalogue of past mass-movement deposits

A total of 149 mass-movement bodies have been identified in the seismic data (64 mass-flow deposits associated to lateral sliding, 19 mass-flow and rotational-slide deposits along the escarpment structure, 51 small wedge-shaped mass accumulation bodies and 15 turbidite deposits). They were mapped and correlated to a total of 21 individual event horizons, each of which was independently dated 1–4 times in different cores (see subsections 3.3.1 and 3.3.3,

Table 3.1: ^{14}C ages and calibration of samples from Lake Zurich.

| Core Nr. | Location ⁽¹⁾ | Depth in core [m] | Sample Nr. | Sample age ⁽²⁾ [^{14}C yr B.P.] | Sample age ⁽³⁾ [cal. yr B.P.] | material |
|--------------------------|-------------------------|----------------------|------------|---|---|--------------|
| ZHK04-1 | 685585 / 240583 | 1.98 | ETH-30711 | 1585 ± 50 | 1350 - 1570 | leaf remains |
| ZHK04-1 | 685585 / 240583 | 3.19 | ETH-30712 | 3230 ± 50 | 3360 - 3570 | leaf remains |
| ZHK04-1 | 685585 / 240583 | 4.6 | ETH-30713 | 4420 ± 60 | 4860 - 5290 | leaf remains |
| ZHK04-1 | 685585 / 240583 | 6.26 | ETH-30762 | 6505 ± 65 | 7270 - 7520 | leaf remains |
| ZHK04-2 | 685744 / 240619 | 2.45 | ETH-30707 | 470 ± 50 | 430 - 560 | leaf remains |
| ZHK04-5 | 699687 / 230486 | 3.38 | ETH-30216 | 5740 ± 70 | 6390 - 6730 | leaf remains |
| ZHK04-5 | 699687 / 230486 | 3.78 | ETH-30215 | 8995 ± 80 | 9750 - 10300 | leaf remains |
| ZHK04-5 | 699687 / 230486 | 4.12 | ETH-30715 | 11560 ± 90 | 13240 - 13640 | wood |
| ZHK04-7 | 688526 / 236159 | 2.07 | ETH-30212 | 1095 ± 50 | 920 - 1150 | leaf remains |
| ZHK04-7 | 688526 / 236159 | 2.81 | ETH-30210 | 2135 ± 55 | 1990 - 2320 | leaf remains |
| ZHK04-7 | 688526 / 236159 | 3.52 | ETH-30213 | 3615 ± 55 | 3820 - 4090 | leaf remains |
| ZHK04-7 | 688526 / 236159 | 4.13 | ETH-30209 | 6105 ± 70 | 6790 - 7170 | leaf remains |
| ZHK04-7 | 688526 / 236159 | 5.03 | ETH-30208 | 8895 ± 80 | 9700 - 10250 | leaf remains |
| ZHK04-7 | 688526 / 236159 | 5.32 | ETH-30206 | 10230 ± 85 | 11600 - 12400 | leaf remains |
| ZHK04-7 | 688526 / 236159 | 5.76 | ETH-30207 | 11710 ± 100 | 13340 - 13770 | wood |
| Zübo 1980 ⁽⁴⁾ | 687615 / 237266 | 5.75 | GL8 | 9990 ± 150 | 11150 - 12100 | wood |
| Zübo 1980 ⁽⁴⁾ | 687615 / 237266 | 7.4 | GL11 | 12400 ± 250 | 13750 - 15250 | wood |
| Zübo 1980 ⁽⁴⁾ | 687615 / 237266 | 7.5 | GL15 | 12800 ± 250 | 14150 - 15850 | wood |
| Zübo 1980 ⁽⁴⁾ | 687615 / 237266 | 9.5 | GL10 | 14150 ± 250 | 16500 - 17300 | wood |
| Zübo 1980 ⁽⁴⁾ | 687615 / 237266 | 13.8 | GL 2 | 14600 ± 250 | 17100 - 18050 | wood |

⁽¹⁾ Location is given in Swiss Grid (CH1903) Coordinates.

⁽²⁾ Dating by AMS (accelerator mass spectrometry) with the tandem accelerator at the Institute of Particle Physics at the Swiss Federal Institute of Technology Zurich (ETH).

⁽³⁾ Calibration (2σ range) was carried out applying the IntCal04-calibration curve (Reimer et al., 2004).

⁽⁴⁾ Dates by Lister (1988).

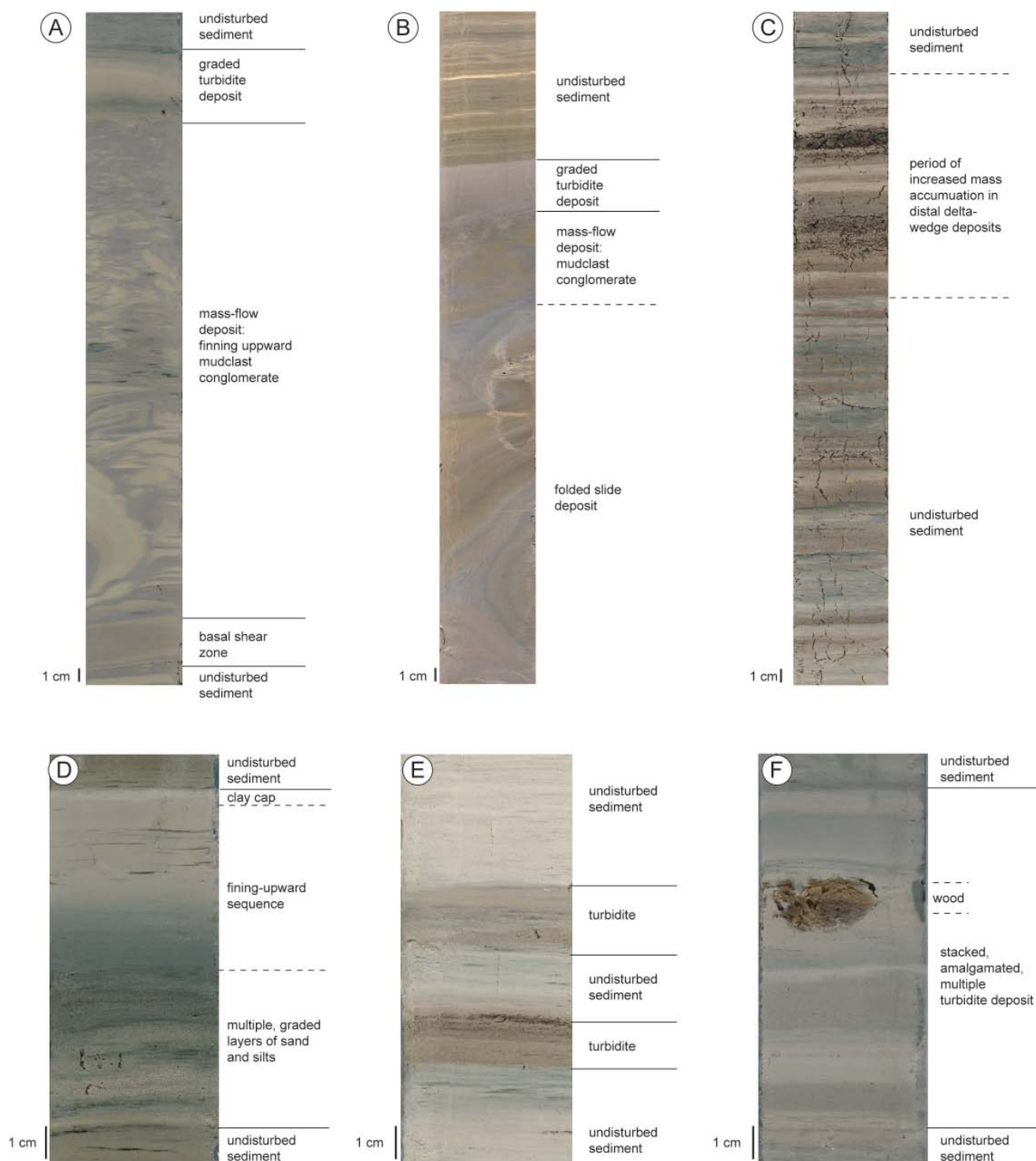


Figure 3.9: Core photos illustrating characteristics of mass-movement deposits in Lake Zurich. A) Core ZHK04-7 (event N): mass-flow and turbidite deposit evolved from translational sliding along the lateral slope. B) Core ZHK04-6 (event Q): slide, mass-flow and turbidite deposit evolved from rotational sliding and longitudinal flow along the escarpment structure. C) Sedimentary succession in core ZHK04-1 showing frequent clastic redeposition layers in a distal deltaic setting. Interval with higher frequency of coarser and thicker layers correlates to a wedge-shaped mass-accumulation body mapped in the seismic data (horizon D). D) Core ZHK04-7 (event K): Turbidite deposit showing multiple layers of sands and silts at the base, a fining-upward sequence and a fine homogeneous clayey cap. E) ZHK04-7 (event J): two small brownish redeposition layers in the lower part of Unit 3a (lacustrine chalk). F) ZHK04-7 (event F): Amalgamation of individual turbidite deposits evolved from multiple, coeval lateral landsliding lacking intercalated undisturbed sediment.

Tab. 3.2). The distribution of mass-movement deposits related to each event horizon (labeled as event A (young) to U (old) according to stratigraphy) are shown in Figure 10. Each of the individual event horizon comprises 1 to 23 mass-movement deposits.

The catalogue of past mass-movement activity in Lake Zurich shown in Figure 3.10 may not be complete because: (1) Limited seismic penetration in the northwestern-most part of the lower Lake Zurich basin, in proximal areas of lateral deltas and in shallow waters did not allow for mapping mass-movement deposits in these area (gray shaded area in Fig. 3.2), (2) relatively small and/or old deposits may not have been recognized due to reworking and deformation by younger and larger events, and (3) only the Holocene deposits were mapped out in the northwestern part of the lower basin due to the fact that the seismic signal did not penetrate into the Late Glacial succession in this area.

3.5 Discussions

The chronological catalogue of Late Glacial-to-Holocene mass-movement deposits together with the identification and characterization of different deposit types in terms of geometry, seismic and sedimentary facies, allows reconstructing an event-based history of slope failure, remobilization and sediment transport processes in peri-alpine Lake Zurich. It furthermore provides the basis for evaluating long-term causes and short-term trigger mechanism of subaquatic landslides in this setting. The following section aims to discuss Lake's Zurich mass-movement event history with respect to different geological processes and impacts that have affected the lake basin over the last ~17000 years.

3.5.1 Human-induced landslides within the last 150 years

During the last 150 years several shore collapses and slumps occurred along the shore of Lake Zurich (e.g. Horgen 1875, Rüschiikon 1898, 1900 and 1907, Oberrieden 1918 and Küssnacht 1943 and 1955 A.D. (NIPKOW 1920; KELTS & HSÜ, 1980; KUEN, 1999)). They directly resulted from human-induced loading of sand and gravel landfill on a weak foundation of lacustrine chalk and have been reported to leave characteristic traces in the sedimentary record of Lake Zurich (NIPKOW, 1920; KELTS, 1978, KELTS & HSÜ, 1980; PIKA, 1984). In the seismic data, mass-movement deposits related to these documented shore collapses can clearly be identified and assigned to corresponding event horizons (events A and B; Note that for the mass-movement deposits near Rüschiikon and Küssnacht it remains unclear, which of the seismically imaged deposits corresponds to which reported event; Fig. 3.10). However, the seismic stratigraphic approach did not allow for assigning individual seismically resolvable event horizons to each of the historically documented events. Therefore they all occur within only two seismic stratigraphic horizons (events A and B) and the mapped

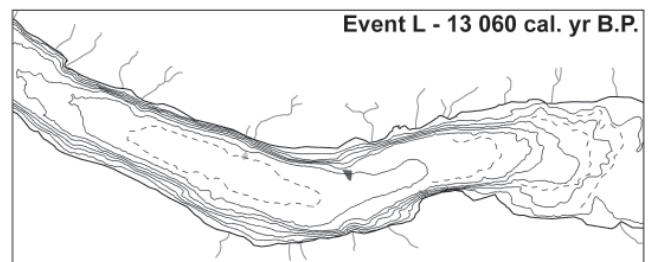
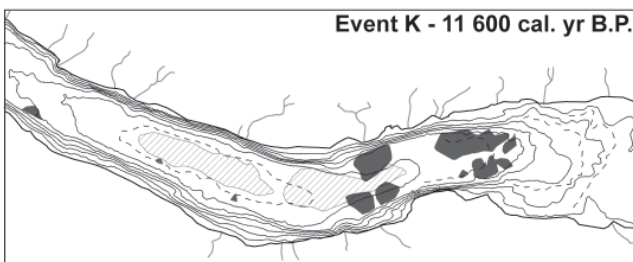
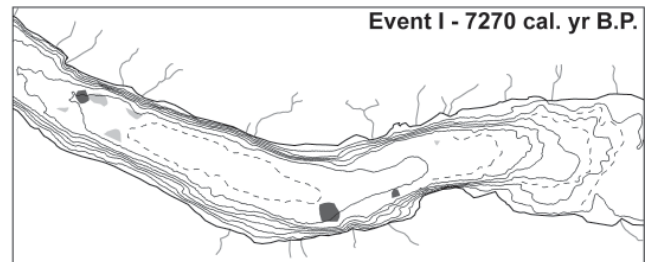
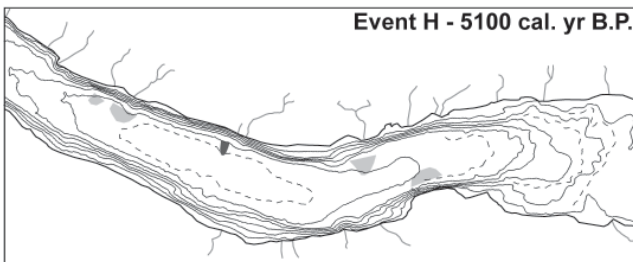
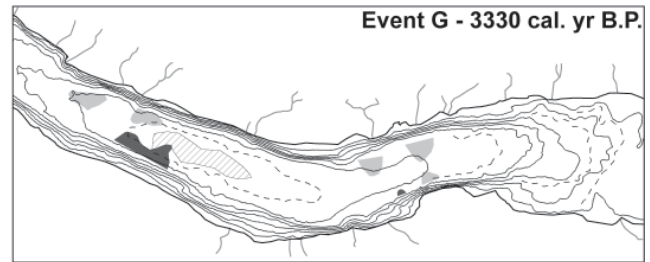
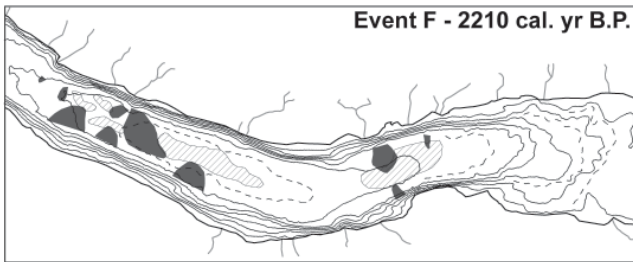
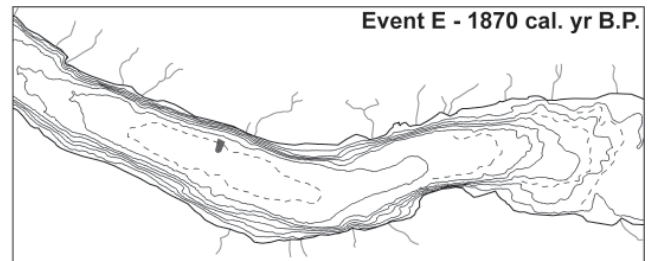
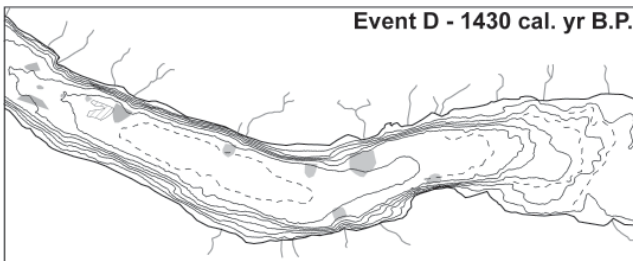
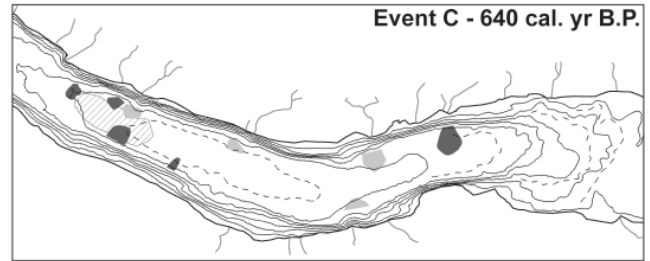
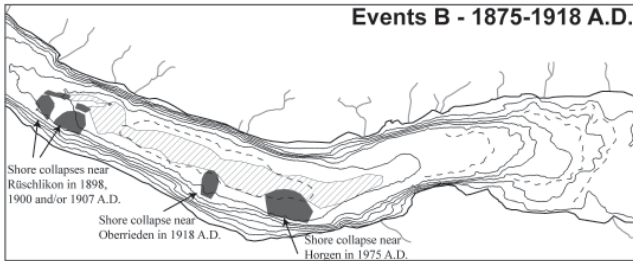
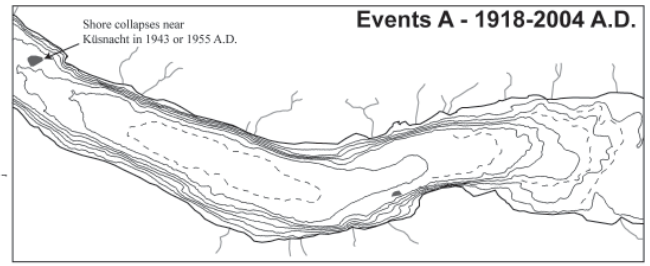
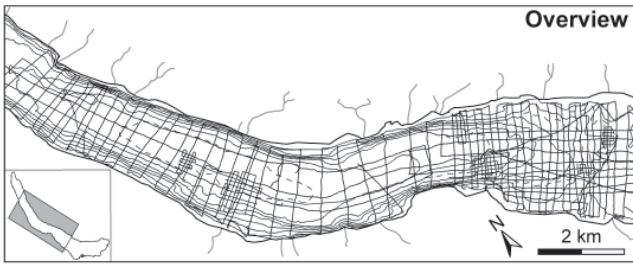
turbidite deposit corresponding to horizon B thus comprise the stacked succession of all events that occurred between 1875 and 1918 A.D..

3.5.2 Events affecting the entire basin («glacial events» and paleo-earthquakes)

One of the most remarkable characteristics of the mass-flow deposits in the subsurface of Lake Zurich is the occurrence of event horizons with multiple coeval mass-flow deposits. 50 of the total 64 mapped mass-flow deposits associated to lateral sliding relate to only 3 event horizons (events F, K and N) and all 19 mass-flow and rotational-slide deposits along the western escarpment of the bedrock high occur only within two event horizons (events Q and U). These outstanding event horizons often also comprise seismically resolvable turbidite deposits, which are characterized in core data by multiple graded sandy layers and amalgamated redeposition layers lacking intercalated undisturbed sediment (Fig. 3.9F). These observations confirm the concurrence of individual landslides and show that regional triggers destabilizing simultaneously the subaquatic slopes repeatedly affected the Lake Zurich area in the past ~17000 years.

The two oldest events (events Q and U) occurred during the transition from the Pleniglacial to the Late Glacial period, when the retreating Linth glacier still was in proximity of Lake Zurich, as indicated by the sedimentary facies of lithologic Unit 1a and b. LISTER (1988) interpreted the transition from Unit 1a to 1b to correspond to the time, when the Linth Glacier retreated back behind the Hurden moraine. During that time, deglaciation of the Linth Glacier has influenced to a large extent sediment input and depositional processes in the upper Lake Zurich basin and along the escarpment structure. High sedimentation rates, potentially punctuated by rapid glacier destabilization phases and/or episodic glacier outburst events, are likely to have influenced slope stability conditions of the glacio-lacustrine deposits. However, whether or not the two rotational sliding events Q and U along the escarpment structure can be related to such episodic «glacial events» remains open.

Alternatively, strong earthquake shaking might be a reliable regional trigger mechanism, as it has been reported in many other studies documenting the relation between synchronicity for a series of subaquatic landslides with strong seismic events that triggered slope failures on a regional scale (e.g., SHILTS and CLAGUE, 1992; SCHNELLMANN, et al., 2002; 2006). Such an earthquake trigger also is the most likely process to explain the occurrence of the three younger event horizons F, K and N, each characterized by at least 10 individual slides along the lateral slopes throughout the lower Lake Zurich basin. In fact, STRASSER et al., (2006) show that all three events correlate to multiple subaquatic landslide deposits in Lake Lucerne. This correlation indicates that three very large earthquakes ($M_w > 6.5$) shook central Switzerland in the past ~15000 years that were strong enough to trigger multiple mass movements in these two lakes located ~40 km apart.



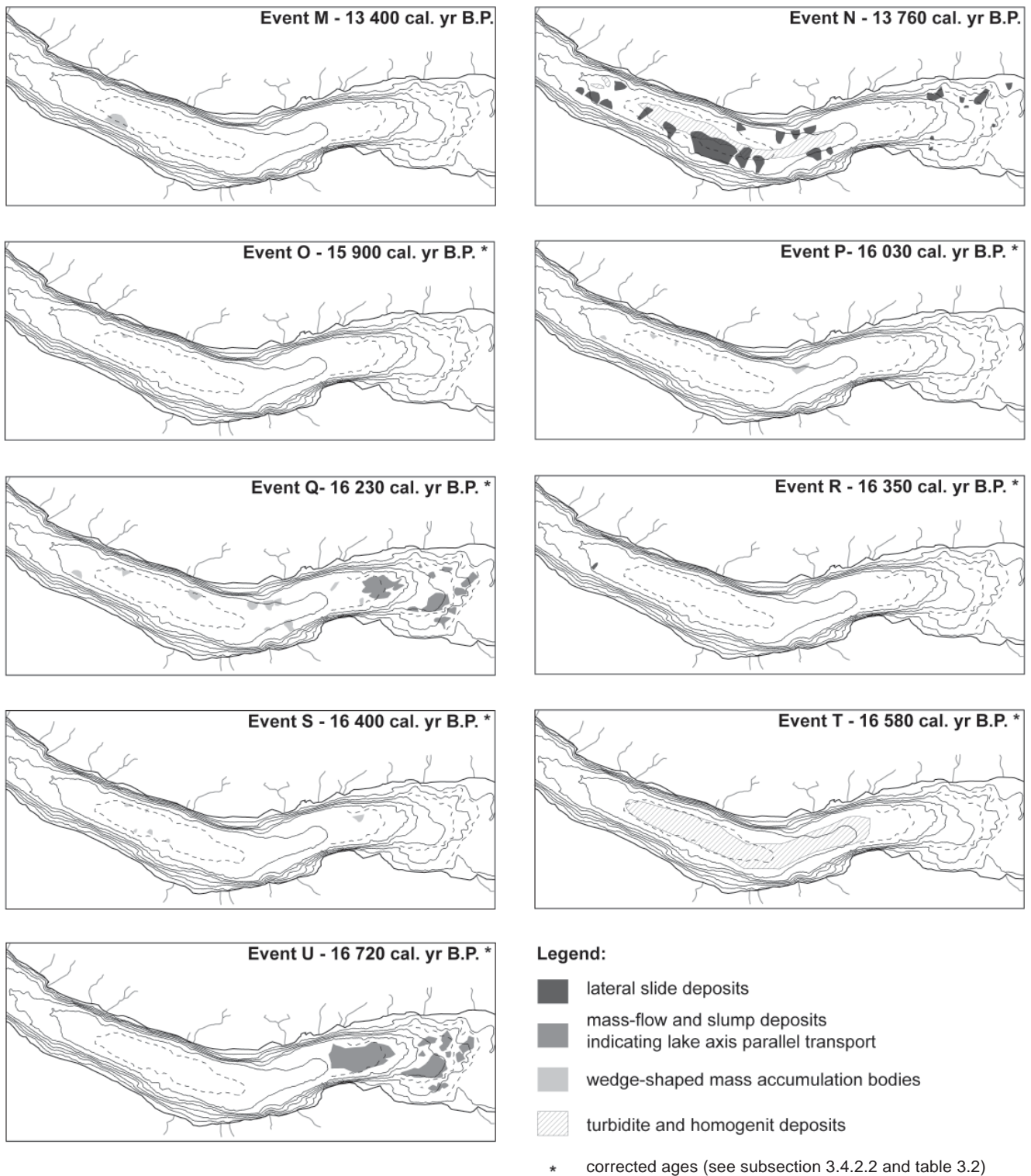


Figure 3.10: Catalogue of mass-movement deposits in the subsurface of Lake Zurich. The upper left panel shows the seismic survey grid, which was used for mapping and correlating the mass-movement deposits. The other panels show the aerial distribution of events A to U as imaged by the seismic data. For dating procedure and age ranges, see Tables 3.1 and 3.2. Asterisks in panel O to U indicate that the age was corrected by 1000 years towards younger ages (see subsection 3.4.2.2 and Table 3.2). Event J cannot be tracked on seismic data and was only observed in core data. It therefore is not included here.

Table 3.2. Dating of prehistoric event horizons.

| Horizon | Sample Nr. | Sample age ⁽¹⁾ | Sample age ⁽²⁾ | Offset ⁽³⁾ | Sed.rate ⁽⁴⁾ | Horizon age | Horizon age (overlap range) | Center of overlap ⁽⁵⁾ | | | | | |
|---------|---------------------|----------------------------|---------------------------|-----------------------|-------------------------|--------------------------------|-----------------------------|----------------------------------|---------------|-------|---------------|---------------|-------|
| Name | | [¹⁴ C yr B.P.] | [cal. yr B.P.] | [cm] | [cm/yr] | [cal. yr B.P.] | [cal. yr B.P.] | [cal. yr B.P.] | | | | | |
| C | ETH-30707 | 470 ± 50 | 430 - 560 | -18 | 0.13 | 569 - 699 | | | | | | | |
| | ETH-30212 | 1095 ± 50 | 920 - 1150 | 46 | 0.14 | 590 - 820 | 590 - 699 | 640 | | | | | |
| D | ETH-30212 | 1095 ± 50 | 920 - 1150 | -21 | 0.06 | 1291 - 1521 | | | | | | | |
| | ETH-30711 | 1585 ± 50 | 1350 - 1570 | 2 | 0.11 | 1331 - 1551 | 1331 - 1521 | 1430 | | | | | |
| E | ETH-30210 | 2135 ± 55 | 1990 - 2320 | 16 | 0.06 | 1707 - 2037 | 1707 - 2037 | 1870 | | | | | |
| F | ETH-30711 | 1585 ± 50 | 1350 - 1570 | -37 | 0.05 | 2092 - 2312 | | | | | | | |
| | ETH-30712 | 3230 ± 50 | 3360 - 3570 | 60 | 0.05 | 2157 - 2367 | | | | | | | |
| | ETH-30210 | 2135 ± 55 | 1990 - 2320 | 3 | 0.06 | 1937 - 2267 | 2157 - 2267 | 2210 | | | | | |
| G | ETH-30213 | 3615 ± 55 | 3820 - 4090 | 24 | 0.04 | 3190 - 3460 | 3190 - 3460 | 3330 | | | | | |
| H | ETH-30713 | 4420 ± 60 | 4860 - 5290 | -2 | 0.07 | 4889 - 5319 | 4889 - 5319 | 5100 | | | | | |
| I | ETH-30209 | 6105 ± 70 | 6790 - 7170 | -3 | 0.03 | 6897 - 7277 | | | | | | | |
| | ETH-30762 | 6505 ± 65 | 7270 - 7520 | 1 | 0.07 | 7255 - 7505 | 7255 - 7277 | 7270 | | | | | |
| J | ETH-30208 | 8895 ± 80 | 9700 - 10250 | - | - | 9700 - 10250 | 9700 - 10255 | 9980 | | | | | |
| K | ETH-30206 | 10230 ± 85 | 11600 - 12400 | 1 | 0.02 | 11534 - 12334 | | | | | | | |
| | ETH-30215 | 8995 ± 80 | 9750 - 10300 | -14 | 0.01 | 11109 - 11659 | | | | | | | |
| | GL8 ⁽⁶⁾ | 9990 ± 150 | 11150 - 12100 | - | - | 11150 - 12100 | 11534 - 11656 | 11600 | | | | | |
| L | ETH-30206 | 10230 ± 85 | 11600 - 12400 | -15 | 0.01 | 12656 - 13456 | 12656 - 13456 | 13060 | | | | | |
| M | ETH-30207 | 11710 ± 100 | 13340 - 13770 | 6 | 0.04 | 13189 - 13619 | 13189 - 13619 | 13400 | | | | | |
| N | ETH-30207 | 11710 ± 100 | 13340 - 13770 | -3 | 0.04 | 13425 - 13855 | | | | | | | |
| | ETH-30715 | 11560 ± 90 | 13240 - 13640 | -5 | 0.03 | 13407 - 13807 | | | | | | | |
| | GL11 ⁽⁶⁾ | 12400 ± 250 | 13750 - 15250 | 5 | 0.04 | 13607 - 15107 | | | | | | | |
| | GL15 ⁽⁶⁾ | 12800 ± 250 | 14150 - 15850 | 15 | 0.04 | 13721 - 15421 | 13721 - 13807 | 13760 | | | | | |
| O | GL10 ⁽⁶⁾ | 14150 ± 250 | 16500 - 17300 | - | - | 16500 - 17300 | 16500 - 17300 | 16900 | | | | | |
| | | | | | | corrected age ⁽⁷⁾ : | 15500 - 16300 | 15900 | | | | | |
| P | GL10 ⁽⁶⁾ | 14150 ± 250 | 16500 - 17300 | -25 | 0.20 | 16625 - 17425 | 16625 - 17425 | 17030 | | | | | |
| | | | | | | corrected age ⁽⁷⁾ : | 15625 - 16425 | 16030 | | | | | |
| Q | GL10 ⁽⁶⁾ | 14150 ± 250 | 16500 - 17300 | -80 | 0.20 | 16900 - 17700 | | | | | | | |
| | | | | | | GL2 ⁽⁶⁾ | 14600 ± 250 | 17100 - 18050 | 100 | 0.20 | 16600 - 17550 | 16900 - 17550 | 17230 |
| | | | | | | corrected age ⁽⁷⁾ : | | | 15900 - 16550 | 16230 | | | |
| R | GL2 ⁽⁶⁾ | 14600 ± 250 | 17100 - 18050 | 45 | 0.20 | 16875 - 17825 | 16875 - 17825 | 17350 | | | | | |
| | | | | | | corrected age ⁽⁷⁾ : | | | 15875 - 16825 | 16350 | | | |
| S | GL2 ⁽⁶⁾ | 14600 ± 250 | 17100 - 18050 | 35 | 0.20 | 16925 - 17875 | 16925 - 17875 | 17400 | | | | | |
| | | | | | | corrected age ⁽⁷⁾ : | | | 15925 - 16875 | 16400 | | | |
| T | GL2 ⁽⁶⁾ | 14600 ± 250 | 17100 - 18050 | - | - | 17100 - 18050 | 17100 - 18050 | 17580 | | | | | |
| | | | | | | corrected age ⁽⁷⁾ : | | | 16100 - 17050 | 16580 | | | |
| U | GL2 ⁽⁶⁾ | 14600 ± 250 | 17100 - 18050 | -600 | 4.29 ⁽⁸⁾ | 17240 - 18190 | 17240 - 18190 | 17720 | | | | | |
| | | | | | | corrected age ⁽⁷⁾ : | | | 16240 - 17190 | 16720 | | | |

⁽¹⁾Dating by AMS (accelerator mass spectrometry) with the tandem accelerator at the Institute of Particle Physics at the Swiss Federal Institute of Technology Zurich (ETH).

⁽²⁾Calibration (2σ range) was carried out applying the IntCal04-calibration curve (Reimer et al., 2004).

⁽³⁾Position of the dated sample relative to the event horizon.

⁽⁴⁾Estimated by linearly interpolating between two ¹⁴C samples after correcting for the thickness of instantaneously deposited turbidite layers.

⁽⁵⁾Ages are rounded to the decade.

⁽⁶⁾Dates by Lister (1988).

⁽⁷⁾Correction of -1300 yrs to account for the likelihood of overestimated ¹⁴C ages (see text section 3.4.2.2).

⁽⁸⁾Sedimentation rates from Zao et al., (1984).

Beside the 5 above mentioned event horizon F, K, N, Q and U that all comprise at least 10 prominent large mass-flow and thick turbidite deposits in the central basin, two identified event horizons are also characterized by more than one evidences for lateral landsliding (event horizon C and D). Event horizon I is associated with 3 small mass-flow deposits in the vicinity of small lateral deltas and event horizon C shows 5 small to medium-sized mass-flow deposits, among which three occur close the deltas. Both horizons are also associated with deltaic wedge-shaped mass accumulation bodies indicating phases of higher remobilization along lateral deltas (see subsection 3.5.3). However, the multiple-deposit pattern might also suggest an earthquake trigger, although strong seismic shaking can be excluded as they would presumably destabilize more slopes at the same time.

Event horizon C is dated to 590–700 cal yr B.P. (1250–1360 A.D.) and might coincide with the M_w 6.9 Basel earthquake in 1356 A.D. (MEGHRAOUI et al, 2001). Macro seismic reconstructions based on historical documents suggest that the northwestern part of Lake Zurich may have experienced macro seismic intensities close to VII (MAYER-ROSA & CADIOT, 1979), which is interpreted to be the threshold intensity for multiple subaquatic landslide initiation (MONECKE et al, 2004; STRASSER et al., 2006). However, an interdisciplinary revision of the 1356 A.D. Basel earthquake rather suggests slightly lower intensities for the study area (FÄH et al., subm.). In any case, the Basel earthquake remains a candidate to have triggered the Lake Zurich event C, because the mass-flow deposits are partly related to slope failures along lateral deltas where threshold stabilities might be lower (see subsection 3.5.3) and delta slopes may have been additionally «charged» by a historically documented super-regional flooding event in 1342 A.D. (SCHWARZ-ZANETTI, 1998).

3.5.3 Deltaic remobilization events during climatic periods of higher clastic sediment supply

Event horizons D, E, G, H, L, M, O, R and S are characterized by either single lateral mass-flow deposits lacking more than one counterpart and/or by wedge-shaped mass accumulation bodies in distal deltaic areas. Given the fact that also the single lateral mass-flow deposits often occur close to lateral deltas these 9 event horizons are interpreted to reflect sediment remobilization events/periods along the lateral deltas. Additionally, periods of higher frequency of exceptional high discharge events in the small catchment and resulting hyperpycnal flows may partly explain the occurrence of the distal deltaic wedge-shaped mass accumulation bodies. For instance, such deposits are also associated with above-mentioned event horizon C (Fig. 3.10) and, hence, might partly be related to the historically documented super-regional flooding event in 1342 A.D. (SCHWARZ-ZANETTI, 1998).

Slope stability conditions of deltas, especially in the proximal area, where the slope is steep, may be relatively close to a critical state where sediment failure may be triggered by only small external disturbances (e.g. weak seismic

shaking) or even can occur spontaneously (GIRARD-CLOS et al, 2007). Reduced stability conditions and thus the likelihood of delta collapse initiation can be caused by a variety of geological processes, among which the two most dominant are: (i) high sedimentation rates increasing the gravitational load and leading to the formation of excess pore pressure (SULTAN et al, 2004) and (ii) biogenic gas production from decomposition of organic material reducing the inter-particle cohesion and friction (COLEMAN & PRIOR, 1988). Both the input of organic material and sedimentation rates are likely to be higher during periods of enhanced precipitation and run-off in the catchment of the small creeks laterally entering Lake Zurich.

The proposed influence of climate-controlled increase of sediment supply as the causing factor for subaqueous delta slope failures in Lake Zurich can be tested by plotting the occurrences of Holocene event horizons C, D, E, G, H, against reconstructed phases of mid-European lake level high-stands interpreted as proxy for higher precipitation and increased river run-off (MAGNY, 2004) (Fig. 3.11). However, the resulting correlation is ambiguous and, therefore, the Lake Zurich dataset does not allow for conclusive interpretation.

3.5.4 Exceptional event layers in Lake Zurich

Two event horizons (J and T) have been identified that are not associated with any mass-flow deposits or wedge-shaped mass accumulation bodies. Event T comprises an up to 1 m-thick deposit characterized by a ponding geometry with internal laterally-continuous very-low-amplitude reflections and thick homogeneous clay deposits in the seismic and core data, respectively (Fig. 3.7). It occurs at the lithological boundary between Unit 1a and 1b which has been interpreted to correspond to the time when the Linth glacier retreated behind the Hurden moraine (LISTER, 1988). Therefore, it is likely that event T is somehow related to the termination of the Hurden Stage, but the physical process of sediment mobilization and deposition remains unknown.

Event J only is defined in cores from the central part of the deep basin (Fig. 3.7) and can not be resolved in the seismic data. It consists of two characteristic 1–2 cm-thick brownish turbidite layers only 2 cm apart (Fig. 3.9E) that occur in the lower part of lithostratigraphic Unit 3a (lacustrine chalk) and that can be correlated as marker beds throughout the deep basin in all cores. Palynological data from core ZHM54 (SIDLER, 1988) show that these two layers comprise high amounts of pre-Quaternary pollen grains indicating a major clastic input from an alpine catchment (HOCHULI, 2004, personal communication). The occurrence of the two characteristic clastic layers thus suggests two exceptional events likely related to exceptional flood events. They may have resulted for instance from outbreaks of a naturally-dammed lake somewhere in the alpine catchment of Lake Zurich, because floods resulting from local high precipitation events may not explain the deposits throughout the lower basin. It remains unclear whether the source of such events may be within the Sihl

catchment (if the Sihl at that time still was discharging into Lake Zurich) or within the catchment of the Linth or Wägital Aa. The latter appears to be less likely as the flood deposits would rather be expected to be deposited in upstream depocentres (e.g. Obersee). However, the two layers of event J are somewhat similar and in comparable stratigraphic position as two exceptional clastic layers described in Lake Constance (SCHNEIDER et al., 2004). These two layers have been interpreted to be related to the failure of two rockslide dams in the catchment area of the Rhein river (deposited by the Flims and Tamins rockslides) and the catastrophically drainage of the landslide-dammed lakes resulting in major floods. However, although it would theoretically be possible that these exceptional flood events could somehow be connected to the catchment area of Lake Zurich (i.e. through the Walensee/Seez valley and the Linth river), the slightly older ages of event J (9700–10250 cal yr B.P.) compared to the age of the Flims rockslide (9460–9490 cal yr. B.P. (DEPLAZES et al., 2007)) and the unlikelihood of clastic material reaching all the way down

to the lower Lake Zurich basin, do not suggest a causal relation between event J and the Flims rockslide.

Among all reconstructed mass-movement events, event N is the most prominent showing 23 individual landslides deposits all over Lake Zurich and it is the only horizon, along which mass-movements deposits have been recovered in all cores (including shallow water cores ZHM52 and ZHK04-5; Fig 3.7). STRASSER et al., 2008 show that this exceptional event horizon furthermore is associated with sediment waves indicating strong currents in the upper flat basin. On the basis of geomorphological and core data in downstream areas of Lake Zurich and of data presented here, STRASSER et al., 2008 interpret that a reconstructed earthquake ~13760 cal yr B.P. may not only have triggered subaquatic landslides all over Lake Zurich but that primary earthquake shaking or secondary effects, such as landslide-generated waves, may have resulted in a sudden collapse of the Zurich moraine leading to a subsequent lake outburst flood lowering the lake level by ~12 m.

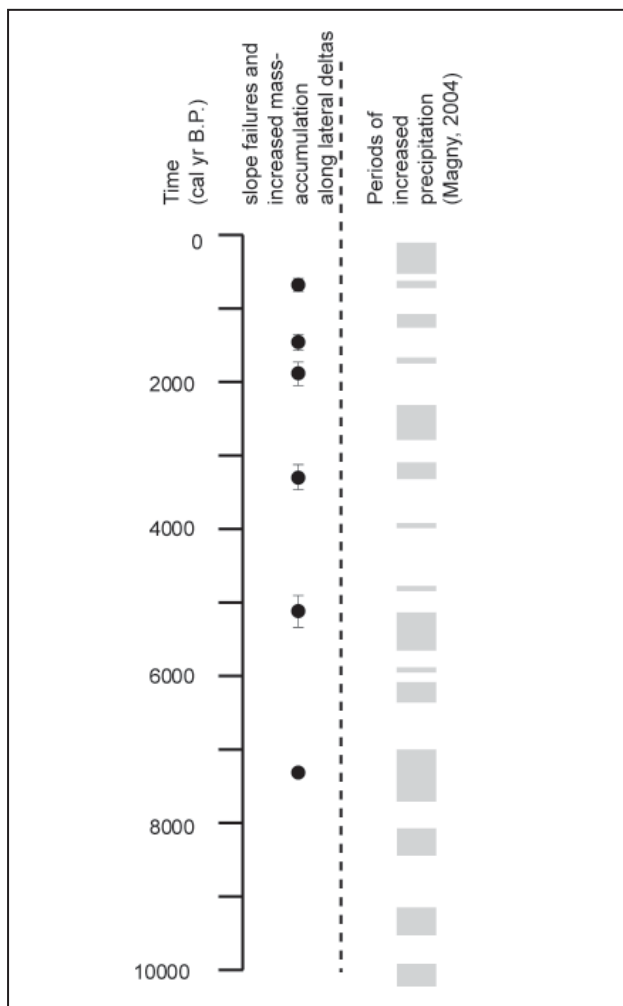


Figure 3.11: Left panel: Stratigraphic distribution of identified mass-movement horizons C, D, E, G, H, and I comprising single lateral mass-flow deposits closed to small lateral deltas and/or distal deltaic wedge-shaped mass-accumulation bodies interpreted to result from increased remobilization and slope failure processes along the delta. Right panel: Gray bars mark reconstructed periods of mid-European lake level high-stands interpreted as proxy for higher precipitation and increased river run-off (MAGNY, 2004).

3.6 Summary and conclusions

The combined basin-wide high-resolution seismic and core study of the subsurface of Lake Zurich enable identification and dating of Late Glacial-to-Holocene mass-movements deposits and allow for determination and characterization of their type, distribution and frequency. The resulting chronological event catalogue presents a record of varying environmental impacts and provides the basis for deciphering seismic vs. climatic trigger mechanism of subaqueous slope failures. Results reveal that a variety of potentially hazardous processes, such as earthquakes, outbursts and floods, affected the study area over the last ~17000 year. The presented mass-movement event stratigraphy provides first information on their frequency and impact, and eventually may yield the means for assessing the geo-hazard potential arising from such natural processes in the densely populated region around Lake Zurich.

A summary list of the main conclusions includes the following:

- (1) 3 major simultaneously-triggered basin-wide lateral slope failure events (translational sliding) occurred at ~2210, 11600 and ~13760 cal yr. B.P. and are interpreted as the fingerprint of strong paleo-seismic activity in the Zurich area.
- (2) Additionally, 2 smaller simultaneously-triggered slope failure events were identified (640 and 7270 cal yr. B.P.), which also might be related to seismic events of lower local intensity. The younger event potentially corresponds to the historic 1356 A.D. Basel earthquake and suggests far-field seismic intensities in the Zurich area, strong enough to trigger subaqueous landslides.
- (3) Two major mass-movement events (rotational sliding) occurred during the transition from the Pleniglacial to the Late Glacial time period and are likely related to the activity of the nearby Linth glacier.
- (4) The record reveals higher frequency of Holocene mass movements in deltaic settings during specific periods that may be related to climate-controlled increase of sediment supply, supposing climatic causing factors for subaqueous delta slope failures.
- (5) Two outstanding event layers, which are not related to lacustrine mass movements, suggest the occurrence of exceptionally high discharge events in the Alpine catchment around 9980 cal yr. B.P.
- (6) The most prominent event layer (dated to 13760 cal yr. B.P.) shows 23 individual landslides deposits all over Lake Zurich and furthermore is associated with sediment waves indicating strong currents in the upper flat basin. These features are interpreted as the fingerprint of an earthquake-triggered collapse of the Zurich moraine dam that resulted in a large outburst of Lake Zurich.

Acknowledgments

We thank Robert Hofmann as well as the whole ETH-Limnoteam and friends for technical support and assistance during the lake campaigns. Many thanks also to Urs Gerber for the core photographs. Stephanie Girardclos, Brian McAdoo, Peter Hochuli, Conrad Schindler and Jiri Pika are acknowledged for helpful discussions on data and interpretations. We thank reviewers Michael Schnellmann and Alex Blass for thoughtful comments that considerably improved the manuscript. This study was supported by the Swiss National Science Foundation (grant 620-066113).

References

- BASTER, I., 2002, Holocene delta in western Lake Geneva and its palaeoenvironmental implications: seismic and sedimentological approach [PhD thesis]: Genève, Université de Genève.
- BONER, M., GEBHARDT, A.C., and PABST, B., 1999, Are Late Glacial Deposits Exposed in Lake Zürich?, Abstract at COL Symposium 1999; Looking into the sediment subsurface of lakes: Zürich.
- BOUMA, A.H., 1987, Megaturbidite - an Acceptable Term: *Geo-Marine Letters*, v. 7, p. 63–67.
- CAMERLENGHI, A., URGELES, R., ERCILLA, G., and BRÜCKMANN, W., 2007, Scientific Ocean Drilling Behind the Assessment of geo-hazards from submarine slides: *Scientific Drilling*, v. 4, p. 45–47.
- CHAPRON, E., BECK, C., POURCHET, M., and DECONINCK, J.F., 1999, 1822 earthquake-triggered homogenite in Lake Le Bourget (NW Alps): *Terra Nova*, v. 11, p. 86–92.
- COLEMAN, J.M., and PRIOR, D.B., 1988, Mass-Wasting on Continental Margins: *Annual Review of Earth and Planetary Sciences*, v. 16, p. 101–119.
- DEPLAZES, G., ANSELMETTI, F.S., and HAJDAS, I., 2007, Lake sediments deposited on the Flims rockslide mass: the key to date the largest mass movement of the Alps, v. 19, p. 252–258.
- FÄH, D., GISLER, M., JAGGI, B., KÄSTLI, P., LUTZ, T., MASCIADRI, V., MATT, C., MAYER-ROSA, D., RIPPMANN, D., SCHWARZ-ZANETTI, G., TAUBER, J., and T., W., submitted, An interdisciplinary Revision of the 1356 Basel Earthquake: submitted to *Geophysical Journal International*.
- GIOVANOLI, F., 1979, Die remanente magnetisierung von Seesedimenten [PhD thesis]: Zürich, ETH Zürich.
- GIRARD-CLOS, S., FIORE, J., RACHOUD-SCHNEIDER, A.M., BASTER, I., and WILDI, W., 2005, Petit-Lac (western Lake Geneva) environment and climate history from deglaciation to the present: a synthesis: *Boreas*, v. 34, p. 417–433.
- GIRARD-CLOS, S., SCHMIDT, O.T., STURM, M., ARIZTEGUI, D., PUGIN, A., and ANSELMETTI, F.S., 2007, The 1996 AD delta collapse and large turbidite in Lake Brienz: *Marine Geology*, v. 241, p. 137–154.
- HEIM, A., 1876, Bericht und Expertengutachten über die im Februar und September 1875 in Horgen vorgekommenen Rutschungen, in *Expertenkommission*, ed., Hofer und Burgen, p. 22.
- HSÜ, K.J., and KELTS, K.R., 1970, Seismic investigation of Lake Zurich; part II, *Geology: Eclogae Geologicae Helveticae*, v. 63, p. 525–538.
- HSÜ, K.J., and KELTS, K.R., 1984, Quaternary geology of Lake Zurich an interdisciplinary investigation by Deep-Lake drilling, *Contribution to Sedimentology: Stuttgart, Schweizerbart*, p. 210.
- HSÜ, K.J., and KELTS, K., 1985, Swiss Lakes as a Geological Laboratory .1. Turbidity Currents: *Naturwissenschaften*, v. 72, p. 315–321.
- HUBER, R., 1938, Der Schuttkegel der Sihl im Gebiete der Stadt Zürich und das prähistorische Delta am See: *Vierteljahresschrift der Naturforschenden Gesellschaft in Zürich*, v. 83, p. 131–214.
- KELTS, K., 1978, Geological and Sedimentary Evolution of Lake Zurich and Zug, Switzerland [PhD thesis]: Zurich, ETH Zurich.
- KELTS, K., and HSU, K.J., 1980, Resedimented facies of 1875 Horgen slumps in Lake Zurich and a process model of longitudinal transport of turbidity currents: *Eclogae Geologicae Helveticae*, p. 73; 1, Pages 271–281.
- KELTS, K., BRIEGEL, U., GHILARDI, K., and HSU, K., 1986, The Limnogeology-EtH Coring System: *Schweizerische Zeitschrift für Hydrologie-Swiss Journal of Hydrology*, v. 48, p. 104–115.
- KUEN, E., 1999, Der Uferabbruch im Kusen: *Küsnachter Jahrheft*, v. 39, p. 44–50.
- LISTER, G.S., 1985, Late Pleistocene Alpine Deglaciation and Post-Glacial Climatic Developments in Switzerland: the record from sediments in a peri-alpine lake basin. [PhD thesis]: Zürich, ETH Zürich.
- LISTER, G.S., 1988, A 15,000-year isotopic record from Lake Zurich of deglaciation and climatic change in Switzerland: *Quaternary Research*, v. 29, p. 129–141.
- LOCAT, J., and LEE, H.J., 2002, Submarine landslides: advances and challenges: *Canadian Geotechnical Journal*, v. 39, p. 193–212.
- LONGVA, O., JANBU, N., BLIKRA, L.H., and BOE, R., 2003, The 1996 Finneidfjord slide; seafloor failure and slide dynamics, in Locat, J., and Mienert, J., eds., *Submarine Mass Movements and their consequences: 1st international Symposium*, p. 531–538.
- MAGNY, M., 2004, Holocene climate variability as reflected by mid-European lake-level fluctuations and its probable impact on prehistoric human settlements: *Quaternary International*, v. 113, p. 65–79.
- MAYER-ROSA, D., and CADIOT, B., 1979, Review of the 1356 Basel Earthquake - Basic Data: *Tectonophysics*, v. 53, p. 325–333.
- MEGHRAOUI, M., DELOUIS, B., FERRY, M., GIARDINI, D., HUGGENBERGER, P., SPOTTKKE, I., and GRANET, M., 2001, Active normal faulting in the upper Rhine graben and paleoseismic identification of the 1356 Basel earthquake: *Science*, v. 293, p. 2070–2073.
- MONECKE, K., ANSELMETTI, F.S., BECKER, A., STURM, M., and GIARDINI, D., 2004, The record of historic earthquakes in lake sediments of Central Switzerland: *Tectonophysics*, v. 394, p. 21–40.
- MULDER, T., and COCHONAT, P., 1996, Classification of offshore mass movements: *Journal of Sedimentary Research*, v. 66, p. 43–57.
- NIESSEN, F., LISTER, G.S., and GIOVANOLI, F., 1992, Dust transport and palaeoclimate during the Oldest Dryas in Central Europe: implications from varves (Lake Constance): *Climate Dynamics*, v. 8, p. 71–81.
- NIPKOW, 1920, Vorläufige Mitteilungen über Untersuchungen des Schlammabsetzes im Zürichsee: *Zeitschrift für Hydrologie*, v. 1, p. 1–28.
- PIKA, J., 1983, Zur Isotopengeochemie und Mineralogie der lacustrinen Ablagerungen im Zürichsee und im Schwarzen Meer [PhD thesis]: Zürich, ETH Zürich.

- PRIOR, D.B., BORNHOLD, B.D., and JOHNS, M.W., 1984, Depositional Characteristics of a Submarine Debris Flow: *Journal of Geology*, v. 92, p. 707–727.
- REIMER, P.J., BAILLIE, M.G.L., BARD, E., BAYLISS, A., BECK, J.W., BERTRAND, C.J.H., BLACKWELL, P.G., BUCK, C.E., BURR, G.S., CUTLER, K.B., DAMON, P.E., EDWARDS, R.L., FAIRBANKS, R.G., FRIEDRICH, M., GUILDERSON, T.P., HOGG, A.G., HUGHEN, K.A., KROMER, B., MCCORMAC, G., MANNING, S., RAMSEY, C.B., REIMER, R.W., REMMELE, S., SOUTHON, J.R., STUIVER, M., TALAMO, S., TAYLOR, F.W., VAN DER PLICHT, J., and WEYHENMEYER, C.E., 2004, IntCal04 terrestrial radiocarbon age calibration, 0–26 cal kyr BP: *Radiocarbon*, v. 46, p. 1029–1058.
- RIESEN, K., and NAEF, F., 2007, What can Neolithic and Bronze Age lake dwellings tell us about former Climate Change?, Abstract at EGU: Vienna.
- SCHINDLER, C., 1968, Zur Quartaergeologie zwischen dem untersten Zuerichsee und Baden: *Eclogae Geologicae Helvetiae*, p. 61; 2, Pages 395–433.
- SCHINDLER, C., 1974, Zur Geologie des Zuerichsees: *Eclogae Geologicae Helvetiae*. 67; 1, Pages 163–196. 1974. 0012-9402.
- SCHINDLER, C., 1976, Eine geologische Karte des Zuerichsees und ihre Deutung: *Eclogae Geologicae Helvetiae*, v. 69, p. 125–138.
- SCHNEIDER, J.-L., POLLET, N., CHAPRON, E., WESSELS, M., and WASSMER, P., 2004, Signature of Rhine Valley sturzstrom dam failures in Holocene sediments of Lake Constance, Germany: *Sedimentary Geology*, v. 169, p. 75–91.
- SCHNELLMANN, M., ANSELMETTI FLAVIO, S., GIARDINI, D., MCKENZIE JUDITH, A., and WARD STEVEN, N., 2002, Prehistoric earthquake history revealed by lacustrine slump deposits: *Geology*, v. 30, p. 1131–1134.
- SCHNELLMANN, M., ANSELMETTI, F.S., GIARDINI, D., and MCKENZIE, J.A., 2005, Mass movement-induced fold-and-thrust belt structures in unconsolidated sediments in Lake Lucerne (Switzerland): *Sedimentology*, v. 52, p. 271–289.
- SCHNELLMANN, M., ANSELMETTI, F.S., GIARDINI, D., and MCKENZIE, J.A., 2006, 15,000 Years of mass-movement history in Lake Lucerne: Implications for seismic and tsunami hazards: *Eclogae Geologicae Helvetiae*, v. 99, p. 409–428.
- SCHWARZ-ZANETTI, G., 1998, Grundzüge der Klima- und Umweltgeschichte des Hoch- und Spätmittelalters in Mitteleuropa [PhD thesis]: Zurich, University of Zurich.
- SHILTS, W.W., and CLAQUE, J.J., 1992, Documentation of earthquake-induced disturbance of lake sediments using subbottom acoustic profiling: *Canadian Journal of Earth Science*, v. 29, p. 1018–1042
- SIDLER, C., 1988, Signification de la palynologie appliquée aux sédiments détritiques et organogènes du Pléistocène supérieur: Eem-Terdiglaciale vürmien et de l'Holocène entre Zoug, Zurich et Baden (Suisse) [PhD thesis]: Zurich, L'Ecole polytechnique fédérale Zurich.
- SIEGENTHALER, C., HSU, K.J., and KLEBOTH, P., 1984, Longitudinal Transport of Turbidity Currents - a Model Study of Horgen Events: *Sedimentology*, v. 31, p. 187–193.
- SIEGENTHALER, C., and STURM, M., 1991, Slump induced surges and sediment transport in Lake Uri, Switzerland, *International Association of Theoretical and Applied Limnology*, Volume 24, p. 955–958.
- SLETTEN, K., BLIKRA, L.H., BALLANTYNE, C.K., NESJE, A., and DAHL, S.O., 2003, Holocene debris flows recognized in a lacustrine sedimentary succession: sedimentology, chronostratigraphy and cause of triggering: *Holocene*, v. 13, p. 907–920.
- STRASSER, M., ANSELMETTI, F.S., FAH, D., GIARDINI, D., and SCHNELLMANN, M., 2006, Magnitudes and source areas of large prehistoric northern Alpine earthquakes revealed by slope failures in lakes: *Geology*, v. 34, p. 1005–1008.
- STRASSER, M., SCHINDLER, C., and ANSELMETTI, F.S., 2008, Late Pleistocene earthquake-triggered moraine dam failure and outburst of Lake Zurich, Switzerland: *Journal of Geophysical Research - Earth Surface*, doi:10.1029/2007JF000802.
- STRASSER, M., STEGMANN, S., BUSSMANN, F., ANSELMETTI, F.S., RICK, B., and KOPF, A., 2007, Quantifying subaqueous slope stability during seismic shaking: Lake Lucerne as model for ocean margins: *Marine Geology*, v. 240, p. 77–97.
- STURM, M., and LOTTER, A.F., 1995, Lake sediments as environmental archives: *EAWAG news*, v. 38, p. 6–9.
- STURM, M., and MATTER, A., 1978, Turbidites and varves in Lake Brienz (Switzerland); deposition of clastic detritus by density currents, in Matter, A., and Tucker, M.E., eds., *Modern and ancient lake sediments; proceedings of a symposium*, Volume Special Publication of the International Association of Sedimentologists. 2, Blackwell. Oxford International. 1978., p. 147–168.
- SULTAN, N., COCHONAT, P., CANALS, M., CATTANEO, A., DENNIELOU, B., HAFLIDASON, H., LABERG, J.S., LONG, D., MIENERT, J., and TRINCARDI, F., 2004, Triggering mechanisms of slope instability processes and sediment failures on continental margins: a geotechnical approach: *Marine Geology*, v. 213, p. 291–321.
- WESSELS, M., 1998, Natural environmental changes indicated by Late Glacial and Holocene sediments from Lake Constance, Germany: *Palaeogeography, Palaeoclimatology, Palaeoecology*, v. 140, p. 421–432.
- ZHAO, X.F., HSUE, K.J., KELTS, K., and KELTS, K.R., 1984, Varves and other laminated sediments of Zuebo, in Hsu, K.J., and Kelts, K.R., eds., *Quaternary geology of Lake Zurich; an interdisciplinary investigation by deep-lake drilling*: Stuttgart, Schweizerbart, p. 161–176.